AD-A135 151 VARIATIONS OF STRONG GROUND MOTIONS IN SIMPLE BASINS FOR EXTERNAL SOURCES(U) SIERRA GEOPHYSICS INC REDMOND WA G R MELLMAN ET AL. 30 NOV 82 AFGL-TR-83-0208 1/1

UNCLASSIFIED F19628-81-C-0044 F/G 8/11 NL

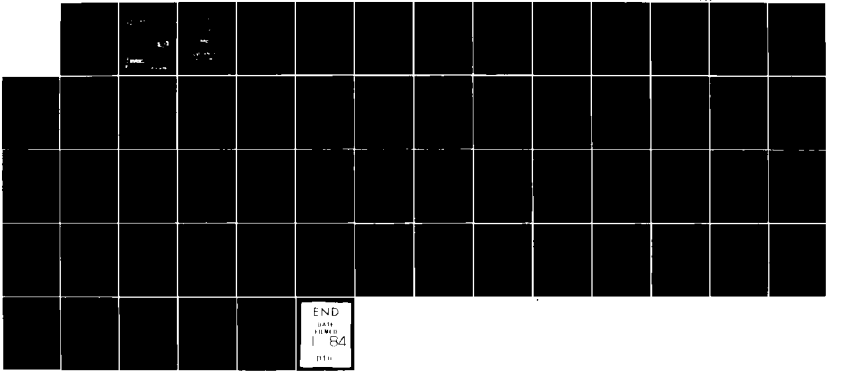

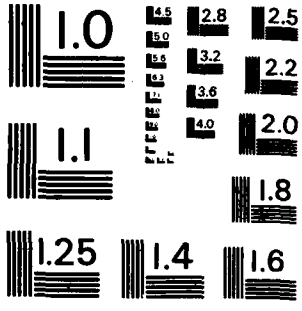

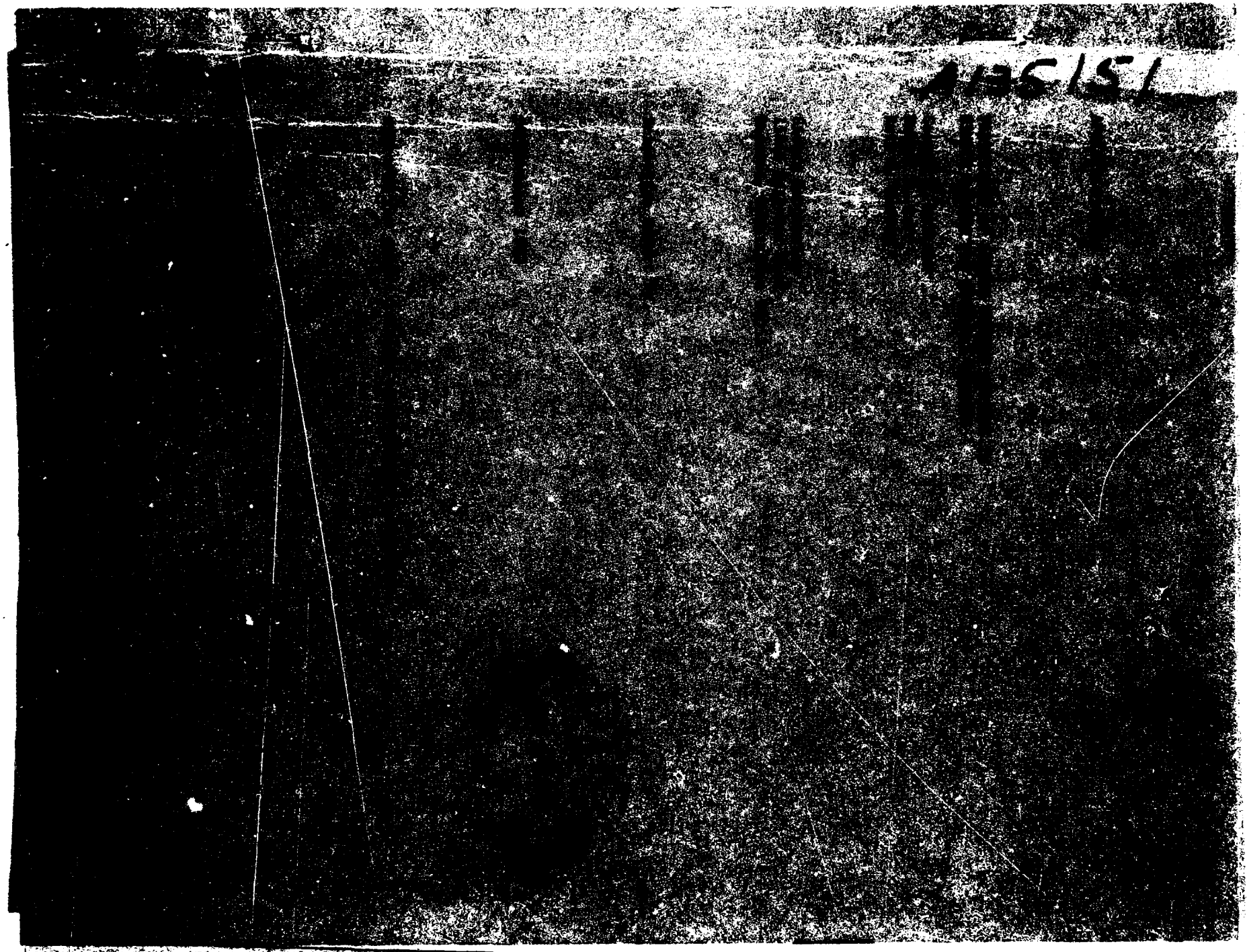
A95/5L

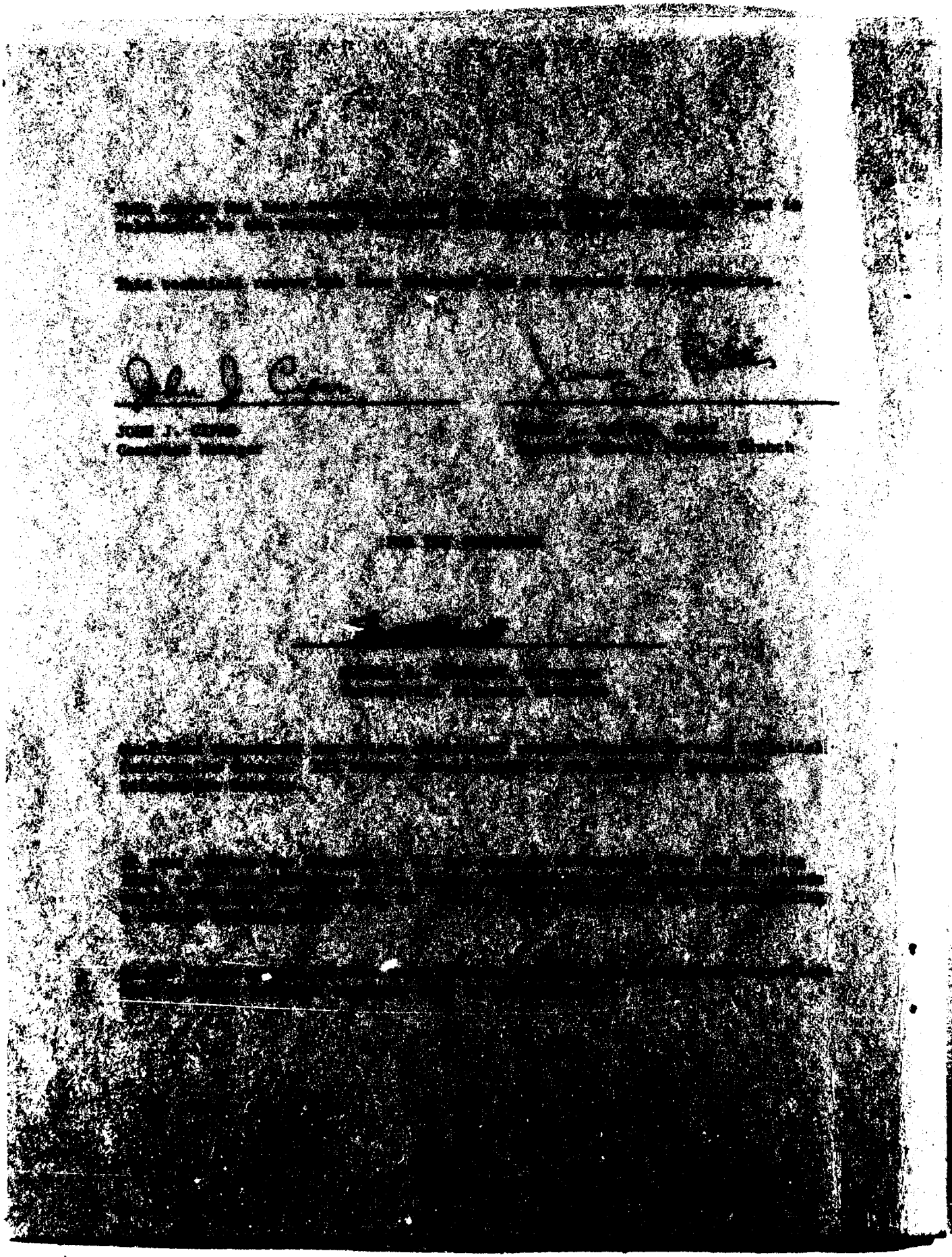

Unclassified

SECURITY CLASSIFICATION OF THIS PAGE (When Data Entered)

REPORT DOCUMENTATION PAGE	READ INSTRUCTIONS BEFORE COMPLETING FORM
1. REPORT NUMBER: AFGL-TR-83-0208	2. GOVT ACCESSION NO.: AD A135151
3. RECIPIENT'S CATALOG NUMBER	
4. TITLE (and Subtitle): VARIATIONS OF STRONG GROUND MOTIONS IN SIMPLE BASINS FOR EXTERNAL SOURCES	5. TYPE OF REPORT & PERIOD COVERED: Scientific Report No. 1
	6. PERFORMING ORG. REPORT NUMBER
7. AUTHOR(s): George R. Mellman, Robert S. Hart, Ruth S. Ludwin	8. CONTRACT OR GRANT NUMBER(s): F19628-81-C-0044
9. PERFORMING ORGANIZATION NAME AND ADDRESS: Sierra Geophysics, 15446 Bell-Red Road, Redmond, Washington 98052	10. PROGRAM ELEMENT, PROJECT, TASK AREA & WORK UNIT NUMBERS: 61102F, 2309G2AG
11. CONTROLLING OFFICE NAME AND ADDRESS: Air Force Geophysics Laboratory, Hanscom AFB, Massachusetts 01731, Monitor/John Cipar/LWH	12. REPORT DATE: 30 November 1982
	13. NUMBER OF PAGES: 59
14. MONITORING AGENCY NAME & ADDRESS (if different from Controlling Office)	15. SECURITY CLASS. (of this report): Unclassified
	15a. DECLASSIFICATION/DOWNGRADING SCHEDULE

16. DISTRIBUTION STATEMENT (of this Report)

Approved for publication; distribution unlimited

17. DISTRIBUTION STATEMENT (of the abstract entered in Block 20, if different from Report)

18. SUPPLEMENTARY NOTES

19. KEY WORDS (Continue on reverse side if necessary and identify by block number)

Strong ground motion

Response spectra variation

20. ABSTRACT (Continue on reverse side if necessary and identify by block number)

The effects of basin shape upon strong ground motion in shallow alluvial basins is examined for a series of simple, geometric basins. The resulting psuedovelocity response spectra contour maps form the basis for the analysis of realistic basin models to be presented in the final report.

DD FORM 1 JAN 73 1473 EDITION OF 1 NOV 65 IS OBSOLETE

Unclassified

SECURITY CLASSIFICATION OF THIS PAGE (When Data Entered)

TABLE OF CONTENTS

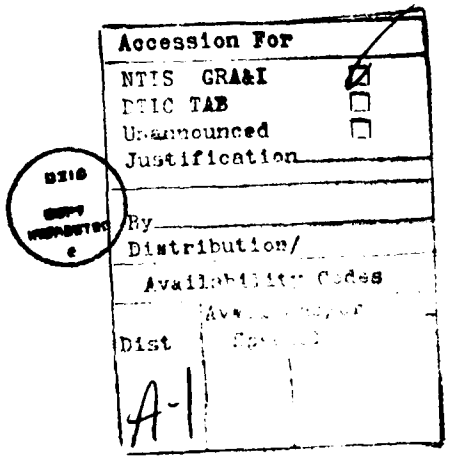

1.0 INTRODUCTION

The goals of this research project are twofold. The first of these is to model the variations in strong ground motion which would be observed in shallow basin structures from sources, both explosions and earthquakes, external to the basin. Also included in that portion of the study is a study of parameter variations (e.g., basin shape, source location) on that strong ground motion. The second task of this project is the development and installation at AFGL of a dynamic ray-tracing computer program which performs these kinds of calculations. Obviously, the development of that program, at least in its basic form, is a necessary step prior to the actual calculational tasks. Much of the effort undertaken during the first 15 months of this project was directed toward the development of that software and indeed efforts to further refine that program still continue. A variety of approaches were examined during this period, the final selection consists of a modification of existing Sierra Geophysics software, originally developed for exploration applications, combined with an efficient and accurate amplitude computation scheme allowing an easy mode of calculation for amplitudes over a wide area. Currently, a local WKBJ approximation is used for amplitude calculations, with a Gaussian beam (Cerveny, et al. 1982) technique under development. A complete discussion of the mathematical and theoretical details of this approach will be included in the final technical report for this project. This report deals solely with the computational results of the basic parameter variation study of the project, the effects of basin shape and depth of source locations, and of frequency variation for a series of five geometrically simple, idealized basin models. In the final technical report, the results of calculations for an actual basin model, that of the NTS basin at Yucca Flats, as well as the contrasting of explosive versus earthquake source type will be presented.

2.0 MODELS

Five different, geometrically simple, basin models were selected in conjunction with the Project Office in order to investigate variations in strong ground motion within basin-like structures. The first two basins were simple elongated structures with semi-circular ends. The two basins differed in the slope of sidewalls the first, referred to as BASIN 1, had 60° sidewalls, the second, referred to as BASIN 5, has 30° slopes. Using the average basin characteristic developed by Battis (1981) for western alluvial basins, the basin lengths were set to be seventy kilometers, the widths were set to be seventeen kilometers, and the maximum depths were 2 kilometers. The compressional wave velocity was 2.90 km/sec, the shear wave velocity 1.67 km/sec, and density 2.2 gm/cc. A map view of the first basin is shown in Figure 1. The surrounding crustal structure was a flat layered structure also derived from Battis (1981). This structure, shown in Figure 2, has four layers above a half-space. Only the top two layers, however, have any significance for this study as reflected energy from deeper horizons would arrive too late and with too little amplitude to have any significance for our purposes. Details of the crustal model are also presented in Figure 2. The second and third models, Basins 2 and 3 respectively, shown in Figures 3 and 4, differ from BASIN 1 and BASIN 5 principally in shape, having one end much narrower giving the models somewhat triangular profiles. In addition, however, BASIN 3 has a linearly sloping basement contact. The depth in this model gradually decreases from two kilometers at the wide end to zero at the narrow end, simulating, in simplified form, an alluvial fan type structure. The last basin type in this study, BASIN 4, shown in Figure 5, is asymmetric, widening by a factor of two halfway along the long axis of the structure. As with the earlier models, this model has a maximum depth of two kilometers and 60° dipping sidewalls. In each case, a series of source locations were chosen, distributed about the basin geometry in a fashion to examine any significant interaction with the basin shape. These source locations are indicated on Figures 1, 3, 4, and 5 by asterisks.

Figure 1. Map view of Basins 1 and 5. Source locations are indicated by stars. Basins 1 and 5 have sidewalls that dip 60° and 30°, respectively. Seismic velocity model is described in the text.

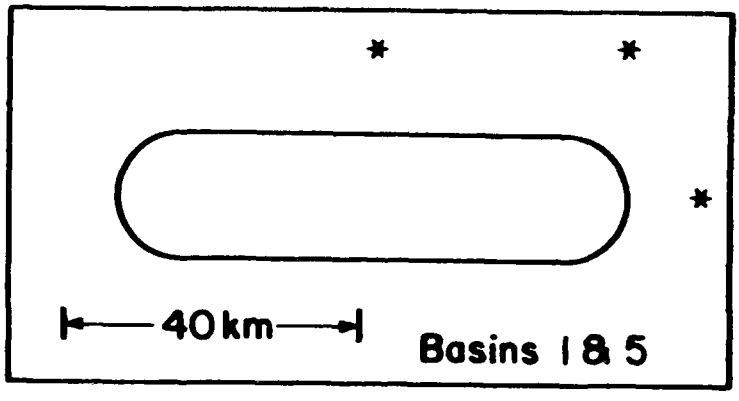

Figure 1

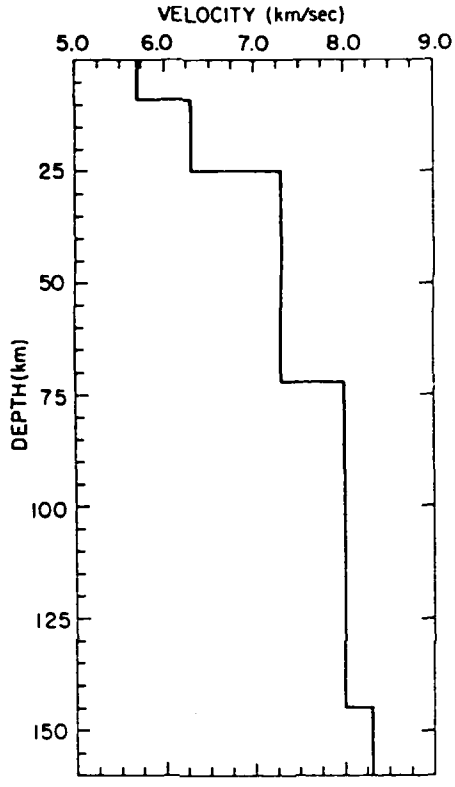

Layer	Thickness (km)	Depth (km)	V_p (km/sec)	V_s (km/sec)
1	9	0	5.7	3.3
2	16	9	6.3	3.6
3	47	25	7.6	4.4
4	73	72	8.0	4.6
5	...	145	8.3	4.8

Figure 2. Crust and upper mantle P-wave velocity structure for the Basin and Range Region (from Battis, 1981).

Figure 3. Map view of Basin 2, a teardrop shape with 60° dipping sidewalls and a flat floor. Stars indicate source locations.

Figure 4. Basin 3 map view, a teardrop shape with a sloping floor. Basement contours at 0.2 km contour interval are shown.

Figure 5. Irregular shaped Basin. See preceding captions and text for description.

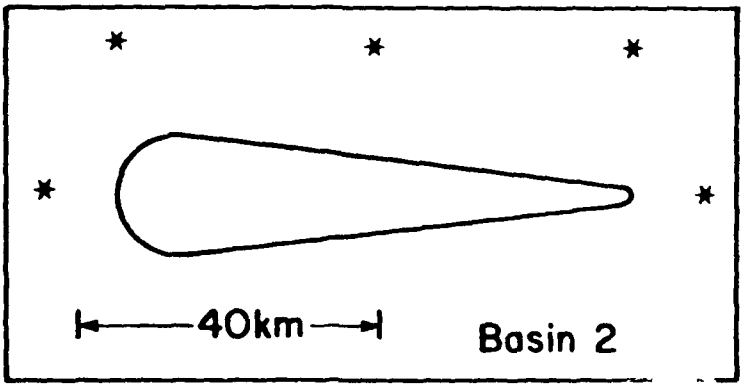

Figure 3

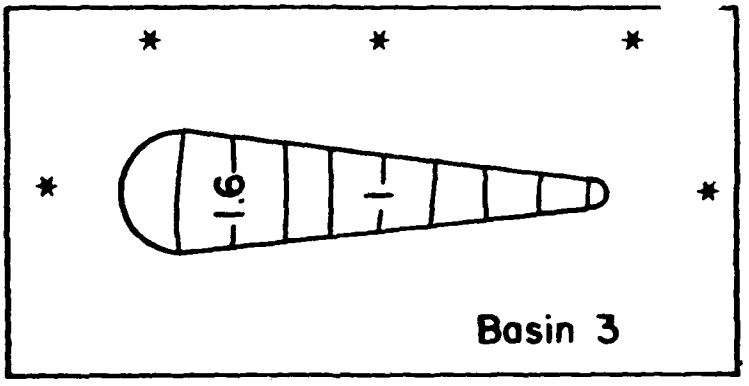

Figure 4

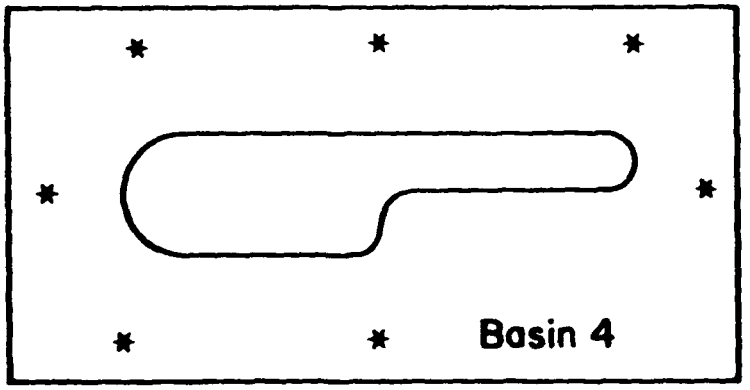

Figure 5

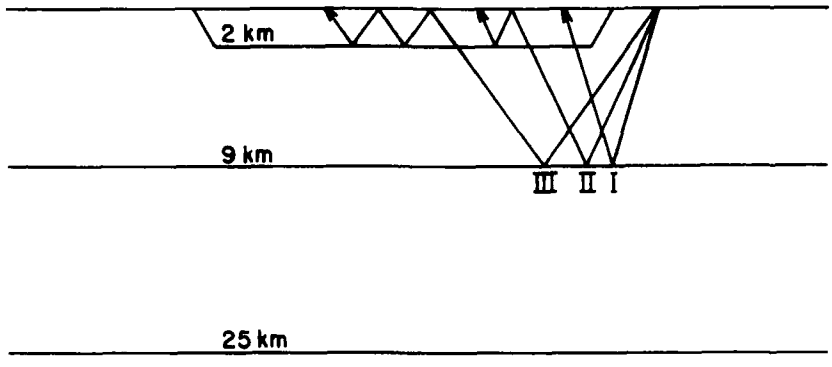

Ray Types I, II, III

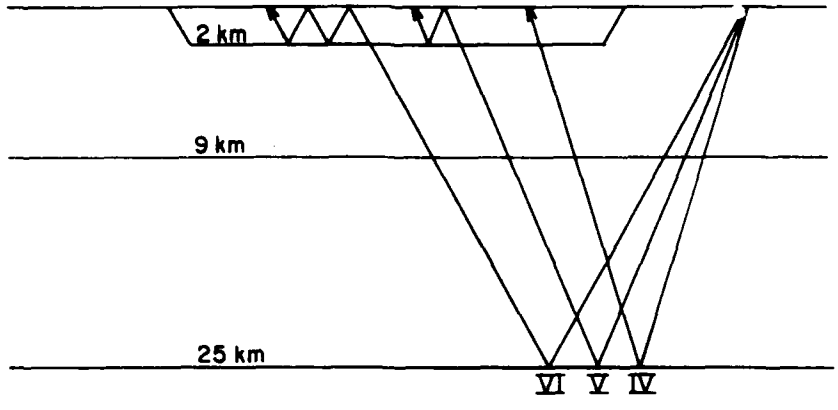

Ray Types IV, V, VI

Figure 6.

It is important to understand the context of the modeling performed using these basin models and the choice of the so-called "average" basin parameters (length, width, depth, sidewall dip, velocities) utilized here. Battis (1981) correctly points out that "the concept of a 'typical' basin model is misleading." The range in such model parameters found in the Basin and Range of the U.S. is quite large. Moreover, the layered structure (and its lateral variation) in each actual basin will differ from all other basins. This last effect has not been included in any of the modeling performed in this project since wavelength considerations indicate its effect to be secondary. It does, of course, influence average velocities. However, our goal here is not to concentrate on details but rather to help understand general effects, to delineate classes of phenomena. Hence we are best served by looking at simple representations of the structures and limiting the parameter variations to one perturbation at a time. Thus we may use our results to be able to confidently characterize the relative effect, and its significance on ground motion, of the particular model feature being perturbed. The end product of this kind of analysis will then be the ability to predict general ground motion effects in specific kinds of basin structure and to formulate a set of guidelines of areas to either seek or avoid. In the remainder of this report, we shall examine a rather large number of maps contouring ground motion for the various basin model-source location combinations shown in the initial figures of this report. The effects of basin shape versus source location for varying frequencies will be discussed. In examining these ground motion contour maps one must remember to concentrate on the gross patterns of variation, not upon specific details. Later, in our final technical report for this project, we shall attempt to utilize these results to interpret the modeling studies on the actual Yucca Flats structure.

3.0 MODELING RESULTS

Complete WKBJ seismograms were computed for a grid of points completely covering the surface area of each basin model. In each case, 40 second time histories were developed with a sample interval of 0.02 seconds. Following the computation of each time history, pseudo-velocity response spectra were computed at each point for frequencies of 0.5 hz, 1.0 hz, 2.0 hz, 4.0 hz, 8.0 hz, and 16.0 hz. The choice of pseudo-velocity response spectra was chosen specifically to be consistent with standard earthquake engineering practice. The response spectrum at a specific frequency, of course, is simply the Fourier spectrum of a particular time history convolved with a damped harmonic oscillator centered at the chosen frequency. In the figures which accompany this section of the report, we have usually only included the 1.0 hz ground motion results unless noticeable frequency dependence of the ground motion intensities was present for the particular basin model-source location pair. The ground motion intensities themselves are plotted as contour maps, each normalized independently to the peak intensity. However, each figure also displays the normalization or scaling factor in order to allow direct comparison of any plot with any other. In all cases, the locations of the sources of the simulated short period ground motion are external to the basins themselves and are positioned at distances outside of the receiver basins at distances corresponding to the typical separations between adjacent basins in the region of interest.

Considerable effort was expended in determining the ray types which produced significant contributions to the ground motion in the receiver basins. With this analysis, it was determined that the significant ground motion could be attributed to six ray types. These are:

Type I : The direct reflection from the first crustal model layer at 9 kilometers.

Type II : Same as Type I but with a single multiple reflection within the basin.

Type III : Same as Type I but with a double multiple reflection within the basin.

Type IV : The direct reflection from the second crustal model layer at 25 kilometers.

Type V : Same as Type IV but with a single multiple reflection within the basin.

Type VI : Same as Type IV but with a double multiple reflection within the basin.

Figure 6 contains a schematic diagram of these six ray types. All of the rays are entirely compressional wave energy. The shear conversions do not materially contribute to the vertical intensities.

BASIN 1

This model is the symmetric, elongated basin with 60° dipping sidewalls. In all of the modeling efforts using this basin, no significant frequency dependence in the spatial distributions of intensities was observed. Ground motion contour maps, at 1.0 hz, are shown in Figures 7, 8, and 9 for three source locations. In each of these plots we can see that the sidewall nearest the source point strongly influences the intensity distribution. In Figures 7 and 8, the high amplitudes are all caused by focusing of Type I rays. Type I rays are also responsible for the band of higher amplitudes observed at the 62 kilometer line in Figure 9. The other two areas of strong ground motion in Figure 9 are Type IV ray focuses.

BASIN 2

The results of modeling BASIN 2, the flat-bottomed, tapered basin model are shown in Figures 10 through 16. Frequency dependence of the ground motion was apparent only when the source was directly offset from the narrow end of the model (Figures 12, 13, and 14). The patterns of intensity are rather more complex in this model relative to

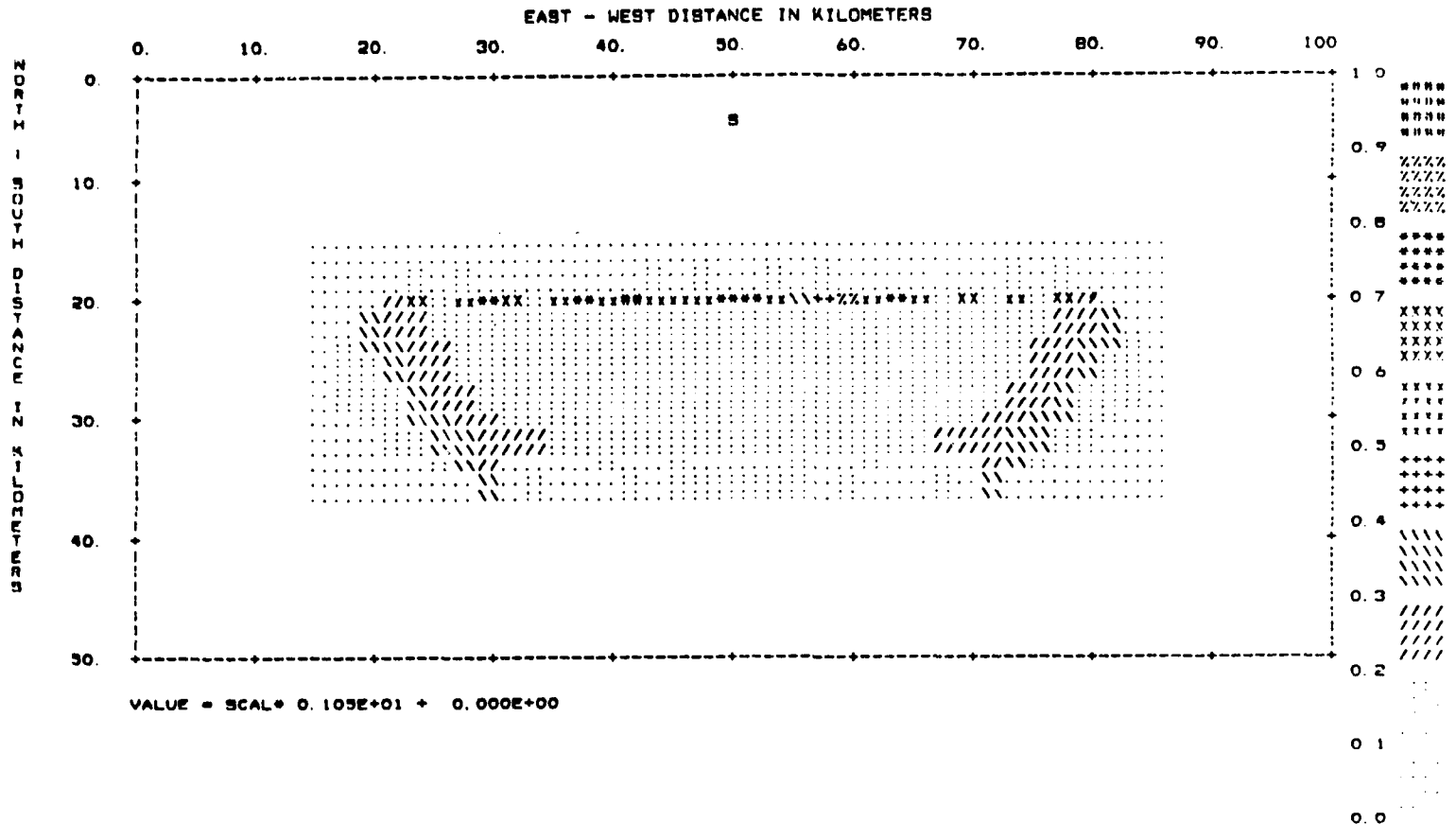
BASIN MODEL 1
PERIOD = 1.0000 SECONDS
EAST - WEST DISTANCE IN KILOMETERS
0.
10.
20.
30.
40.
50.
60.
70.
80.
90.
100
NORTH - SOUTH DISTANCE IN KILOMETERS
0.
10.
20.
30.
40.
50.
S
1.0
0.9
0.8
0.7
0.6
0.5
0.4
0.3
0.2
0.1
0.0
VALUE = SCALE 0.105E+01 + 0.000E+00

FIGURE 7

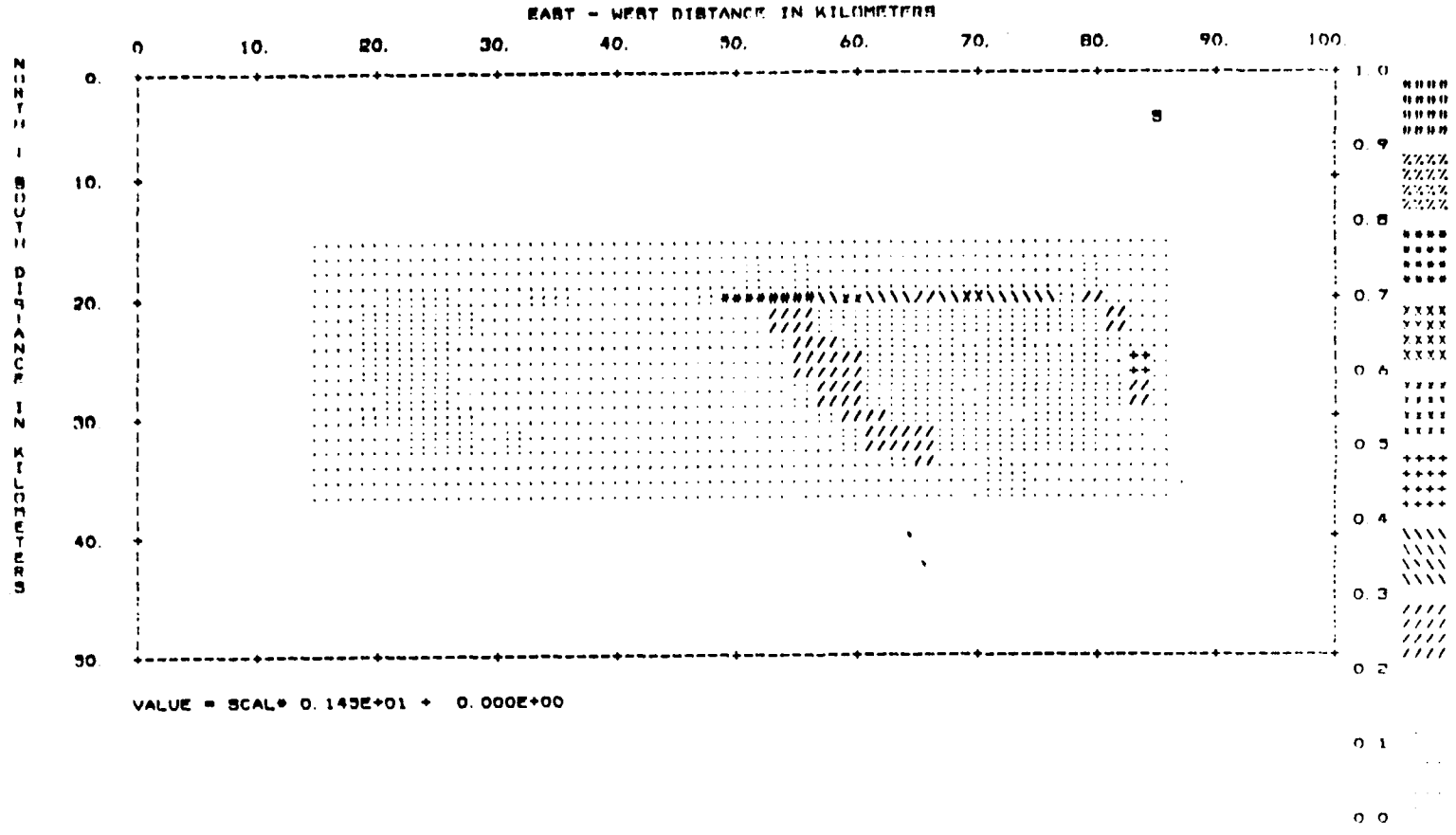
BASIN MODEL 1
PERIOD = 1.0000 SECONDS
EAST - WEST DISTANCE IN KILOMETERS
0
10.
20.
30.
40.
50.
60.
70.
80.
90.
100
NORTH - SOUTH DISTANCE IN KILOMETERS
0.
10.
20.
30.
40.
50.
1.0
0.9
0.8
0.7
0.6
0.5
0.4
0.3
0.2
0.1
0.0
VALUE = SCALE 0.145E+01 + 0.000E+00

FIGURE 8

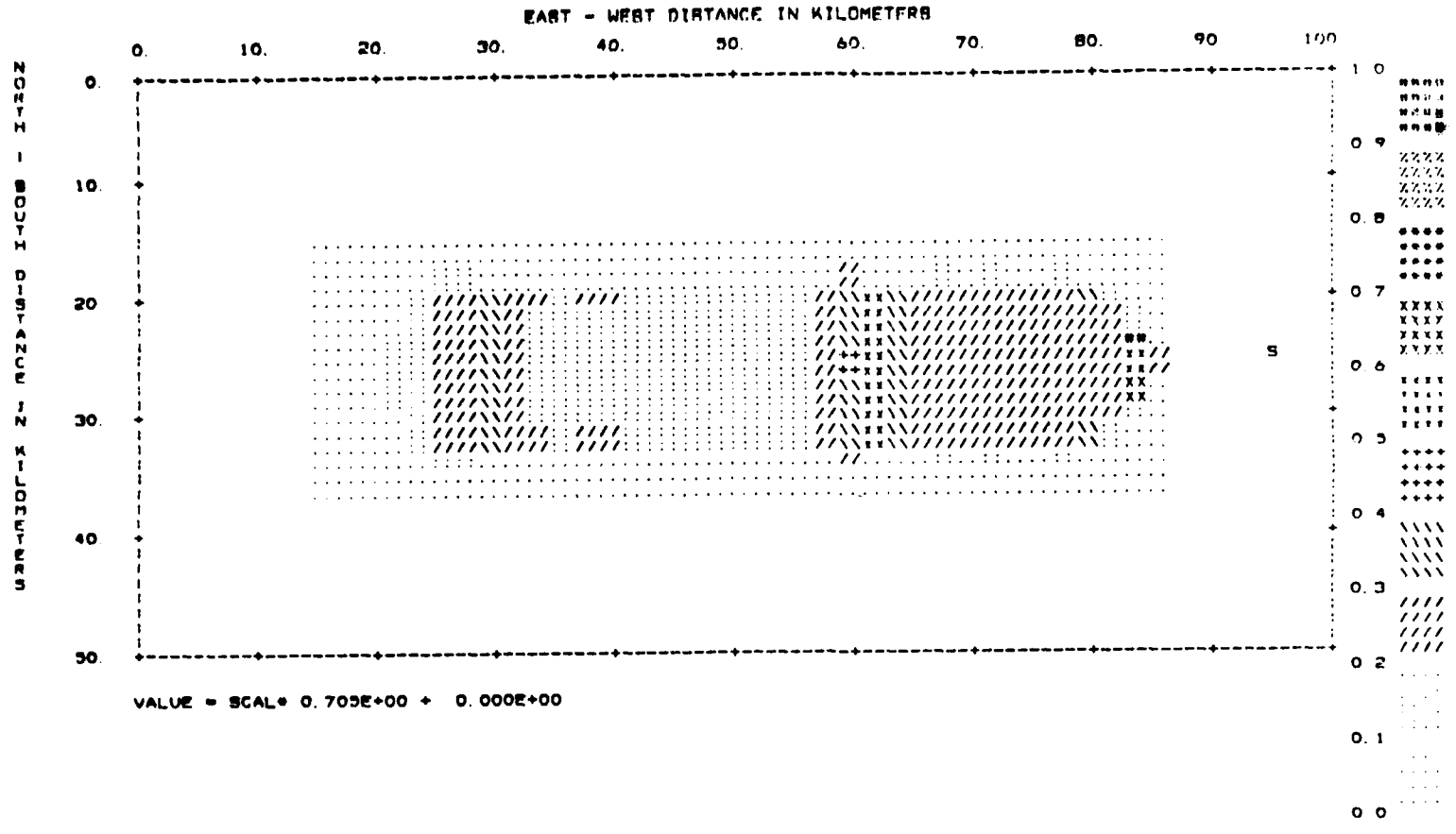
BASIN MODEL 1
PERIOD = 1.0000 SECONDS
EAST - WEST DISTANCE IN KILOMETERS
0.
10.
20.
30.
40.
50.
60.
70.
80.
90
100
NORTH - SOUTH DISTANCE IN KILOMETERS
0.
10.
20.
30.
40.
50.
S
1.0
0.9
0.8
0.7
0.6
0.5
0.4
0.3
0.2
0.1
0.0
VALUE = SCALE 0.705E+00 + 0.000E+00

FIGURE 9

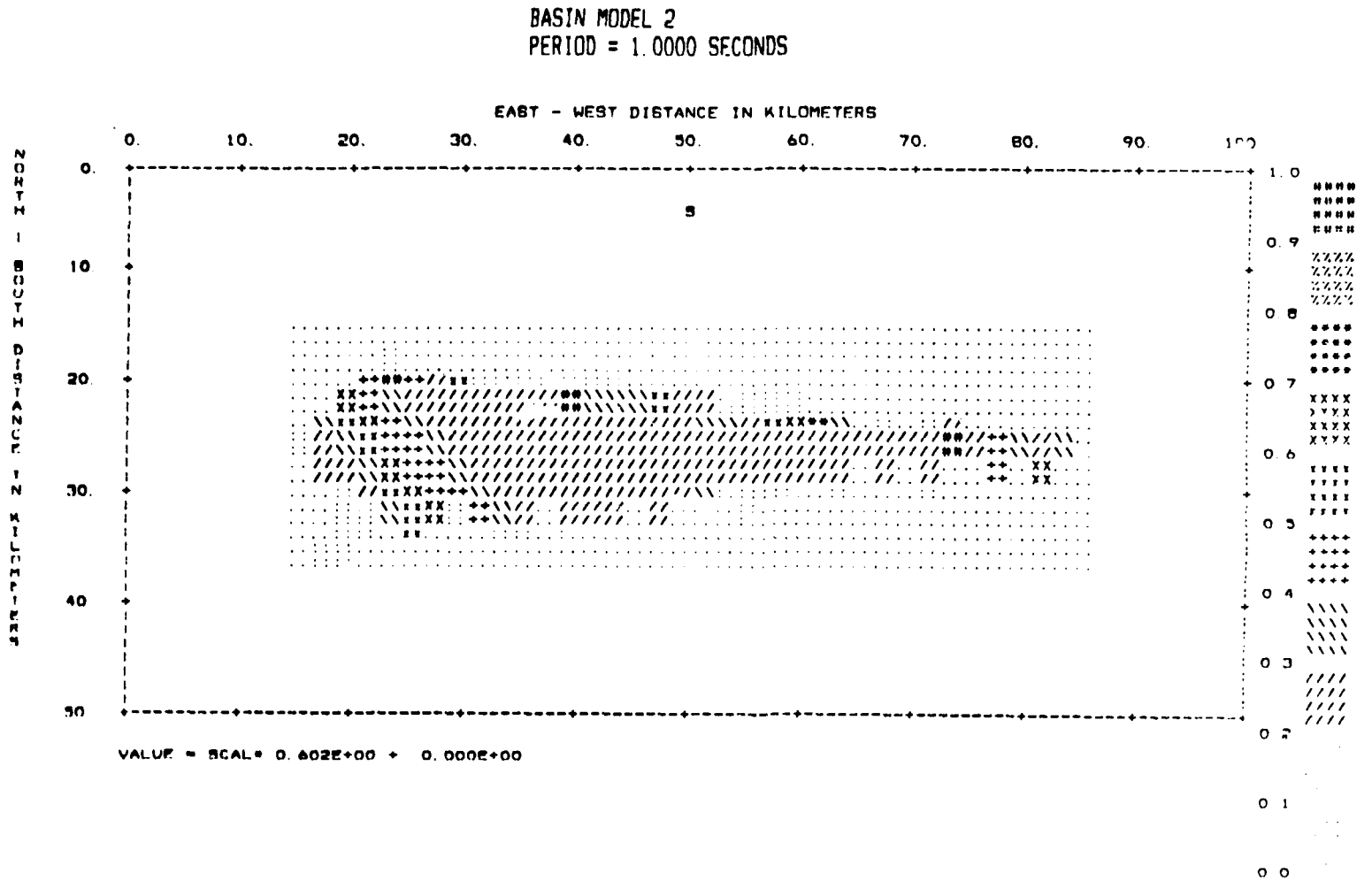
BASIN MODEL 2
PERIOD = 1.0000 SECONDS
EAST - WEST DISTANCE IN KILOMETERS
0.
10.
20.
30.
40.
50.
60.
70.
80.
90.
NORTH - SOUTH DISTANCE IN KILOMETERS
0.
10
20.
30.
40
50
S
1.0
0.9
0.8
0.7
0.6
0.5
0.4
0.3
0.2
0.1
0.0
VALUE = SCALE 0.602E+00 + 0.000E+00

FIGURE 10

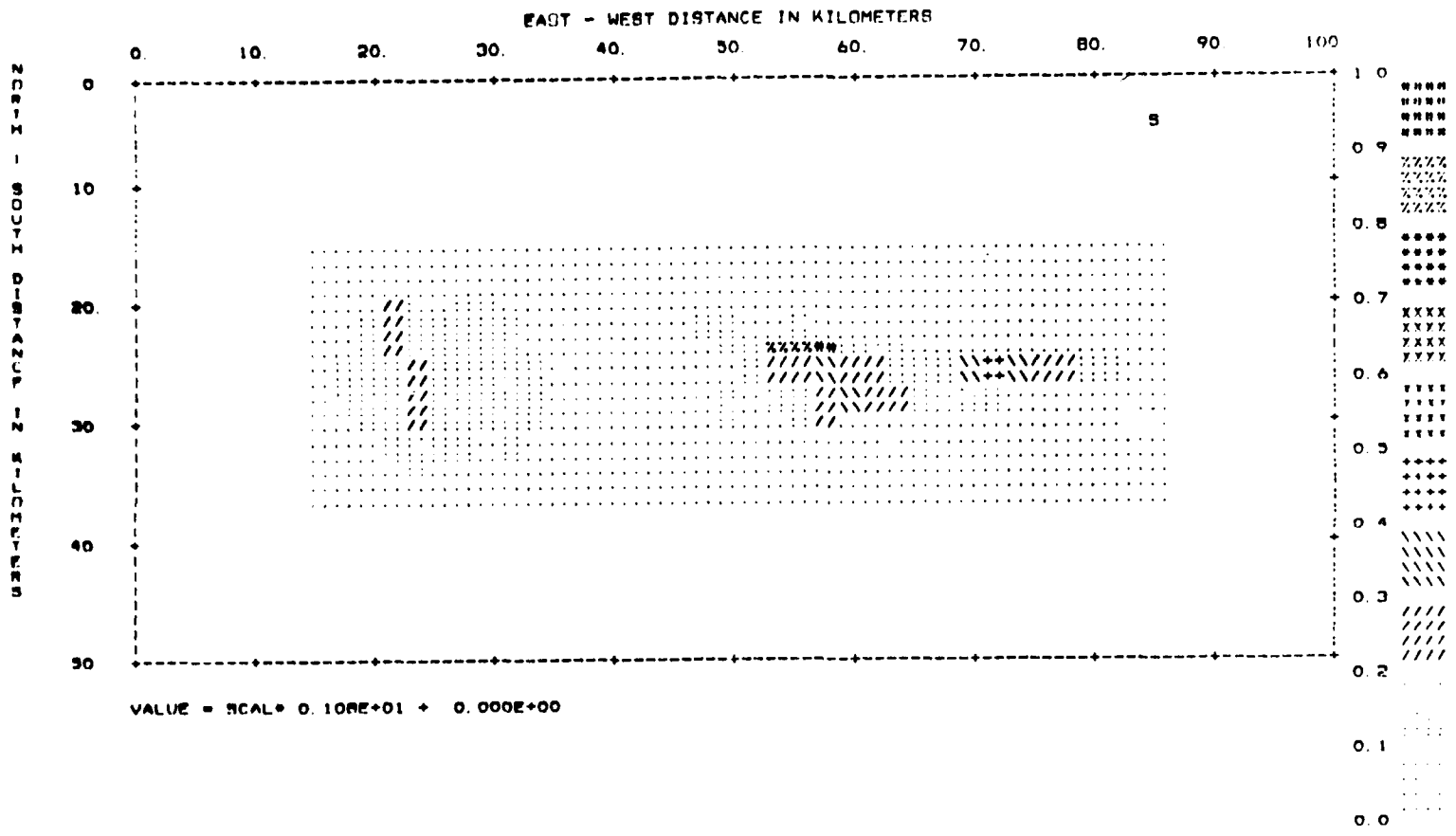
BASIN MODEL 2
PERIOD = 1.0000 SECONDS
EAST - WEST DISTANCE IN KILOMETERS
0. 10. 20. 30. 40. 50. 60. 70. 80. 90. 100
NORTH - SOUTH DISTANCE IN KILOMETERS
0 10 20 30 40 50
S
1.0 0.9 0.8 0.7 0.6 0.5 0.4 0.3 0.2 0.1 0.0
VALUE = SCALE 0.10E+01 + 0.00E+00

FIGURE 11

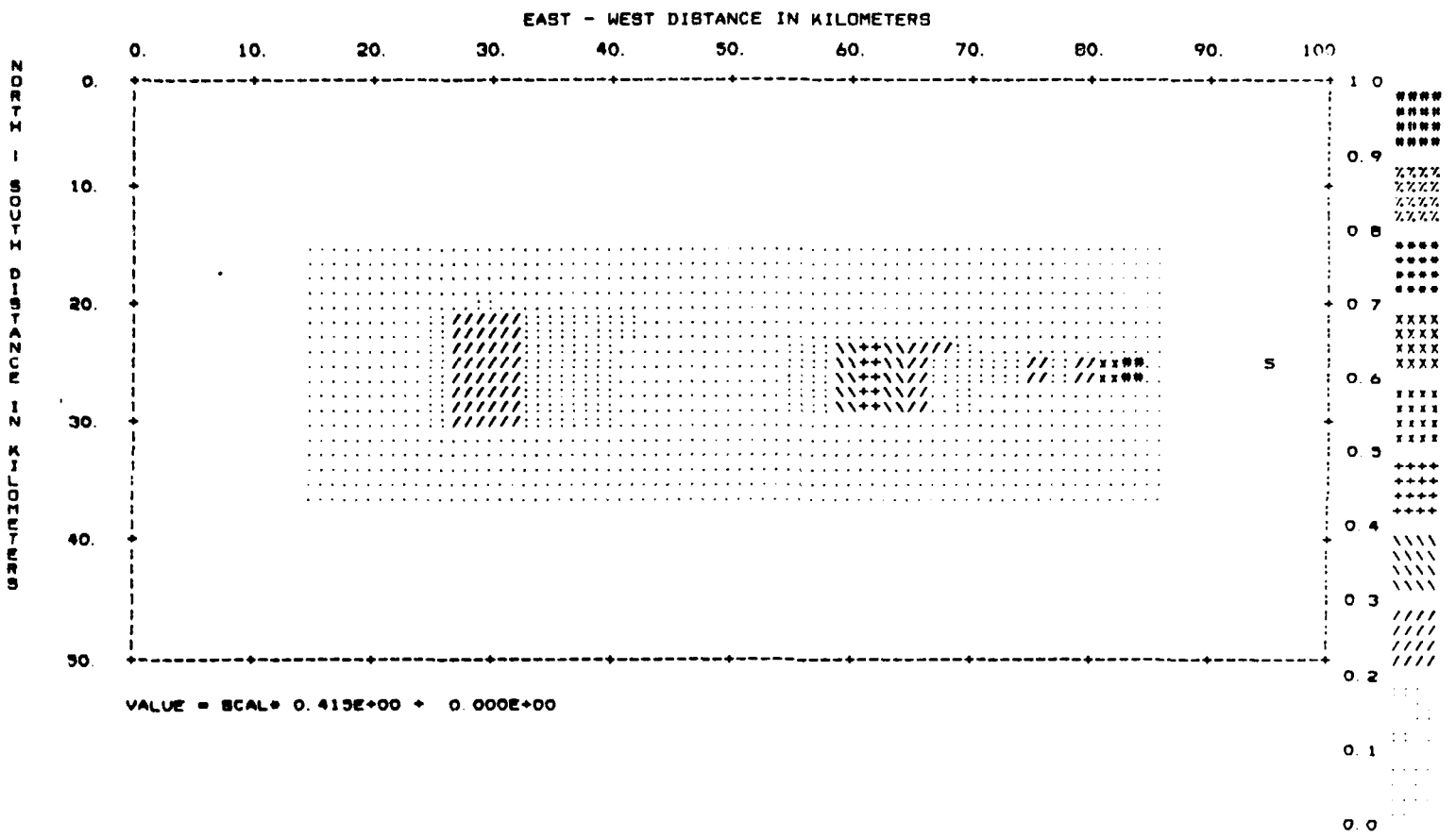
BASIN MODEL 2
PERIOD = 2.0000 SECONDS
EAST - WEST DISTANCE IN KILOMETERS
0. 10. 20. 30. 40. 50. 60. 70. 80. 90. 100
NORTH - SOUTH DISTANCE IN KILOMETERS
0. 10. 20. 30. 40. 50.
1.0 0.9 0.8 0.7 0.6 0.5 0.4 0.3 0.2 0.1 0.0
S
VALUE = SCALE 0.415E+00 + 0.000E+00

FIGURE 12

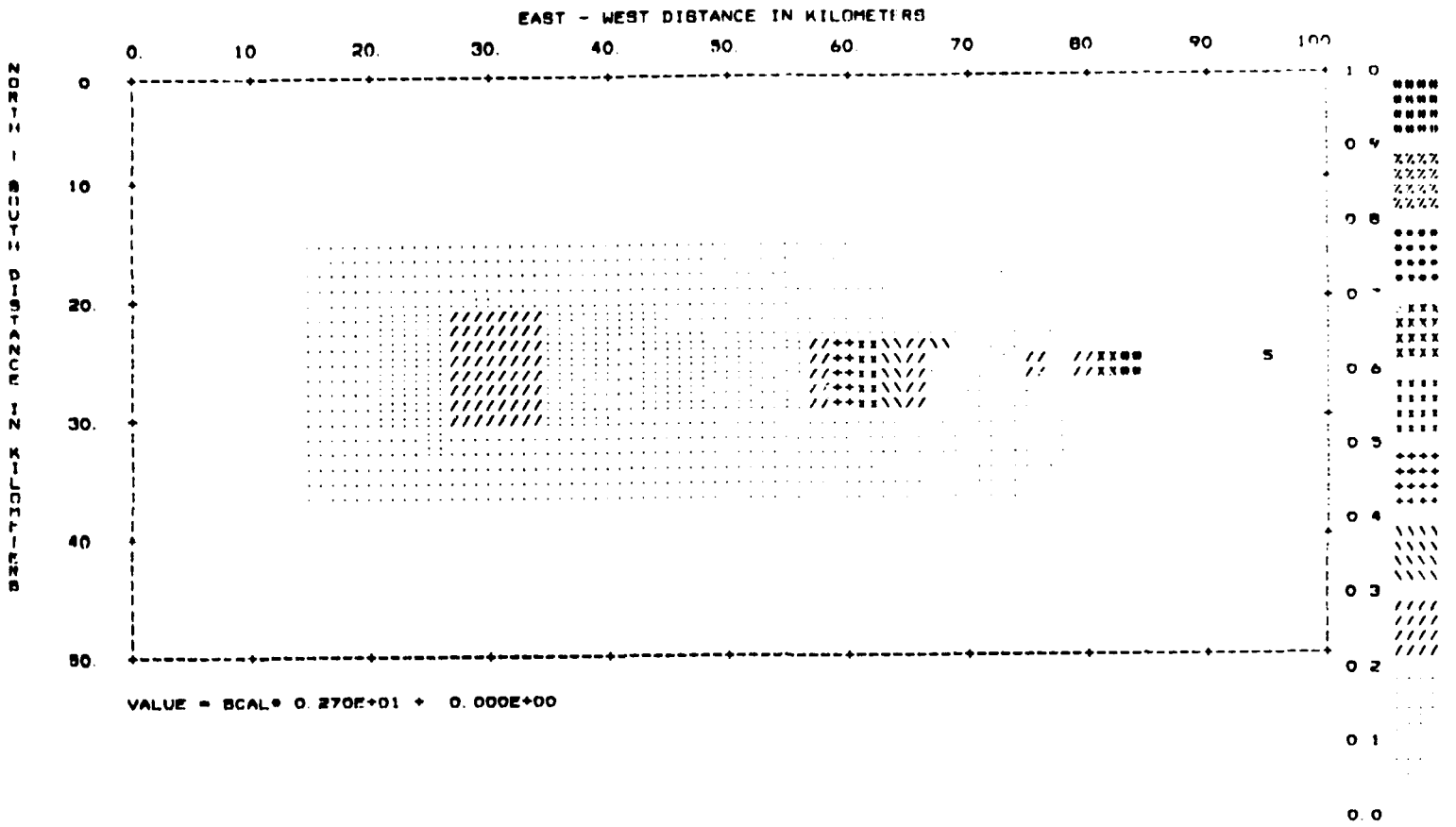
BASIN MODEL 2
PERIOD = 0.5000 SECONDS
EAST - WEST DISTANCE IN KILOMETERS
0.
10
20.
30.
40.
50
60
70
80
90
100
NORTH - SOUTH DISTANCE IN KILOMETERS
0
10
20.
30.
40
50.
1.0
0.9
0.8
0.7
0.6
0.5
0.4
0.3
0.2
0.1
0.0
5
VALUE = BCAL* 0.270E+01 + 0.000E+00

FIGURE 13

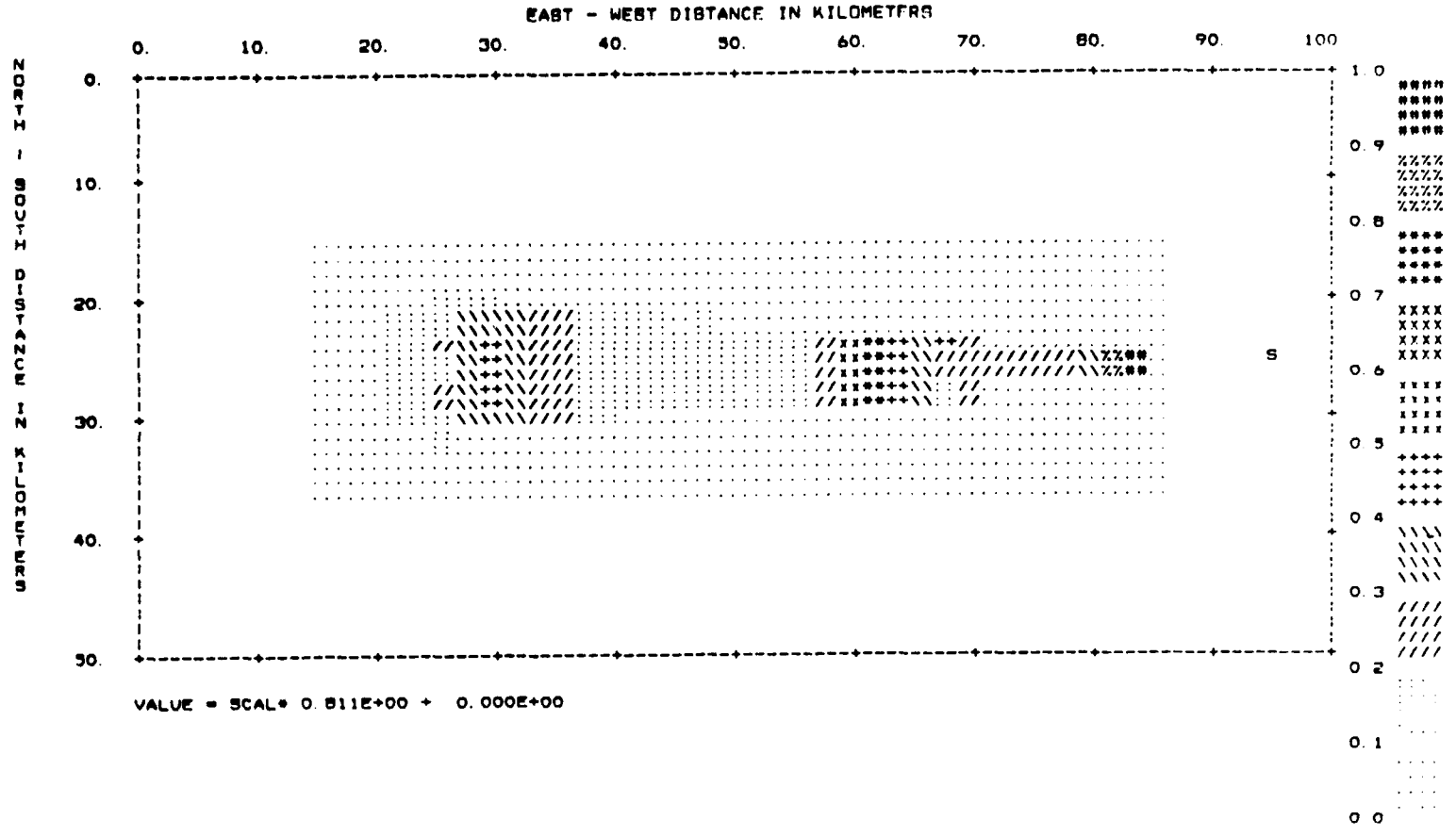
BASIN MODEL 2
PERIOD = 0.0625 SECONDS
EAST - WEST DISTANCE IN KILOMETERS
0. 10. 20. 30. 40. 50. 60. 70. 80. 90. 100
NORTH - SOUTH DISTANCE IN KILOMETERS
0. 10. 20. 30. 40. 50.
1.0 0.9 0.8 0.7 0.6 0.5 0.4 0.3 0.2 0.1 0.0
S
VALUE = SCALE 0.811E+00 + 0.000E+00

FIGURE 14

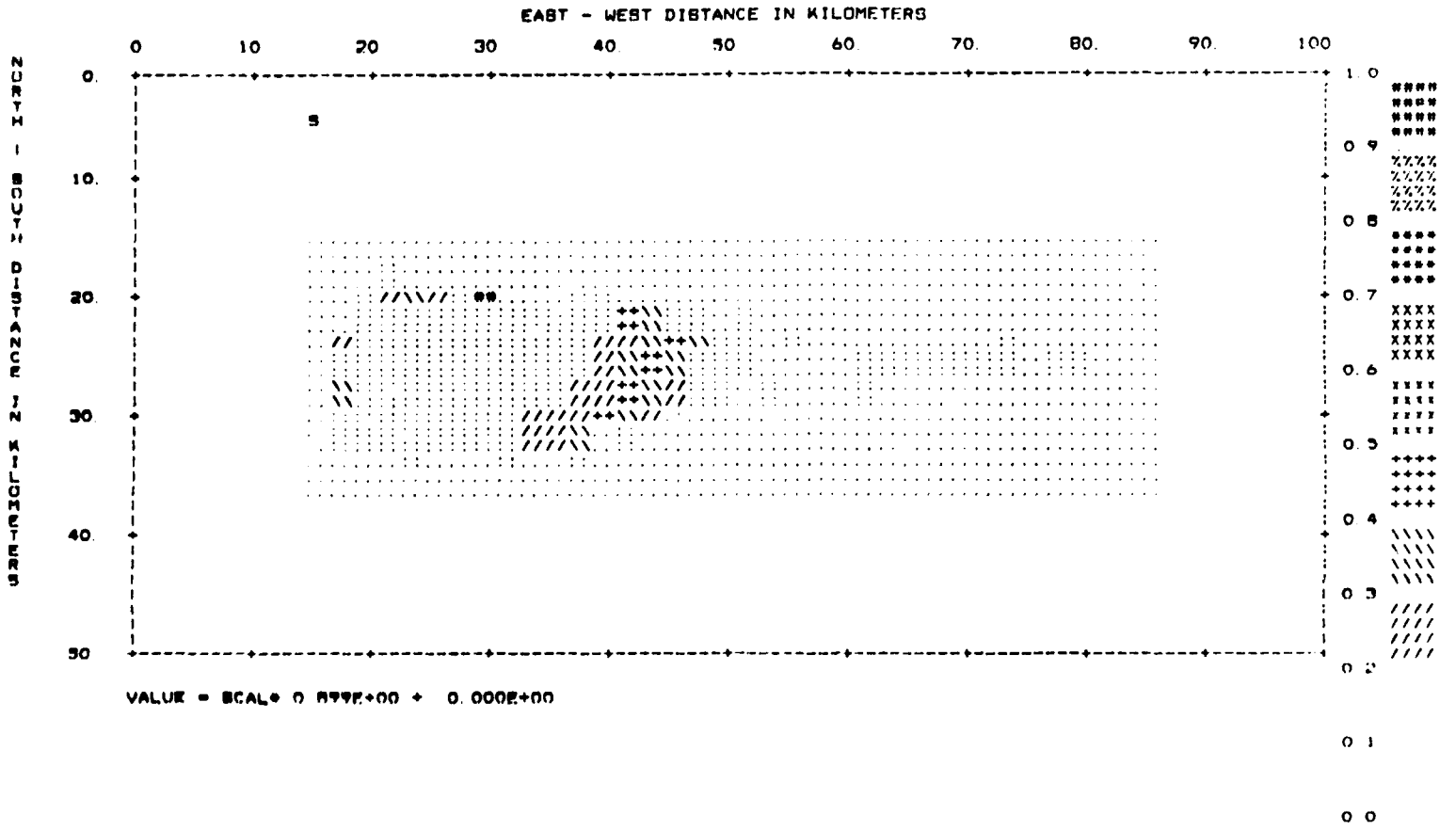
BASIN MODEL 2
PERIOD = 1.0000 SECONDS
EAST - WEST DISTANCE IN KILOMETERS
0
10
20
30
40
50
60
70
80
90
100
NORTH - SOUTH DISTANCE IN KILOMETERS
0.
10.
20.
30.
40.
50
1.0
0.9
0.8
0.7
0.6
0.5
0.4
0.3
0.2
0.1
0.0
VALUE = SCALE 0.8888E+00 + 0.000E+00

FIGURE 15

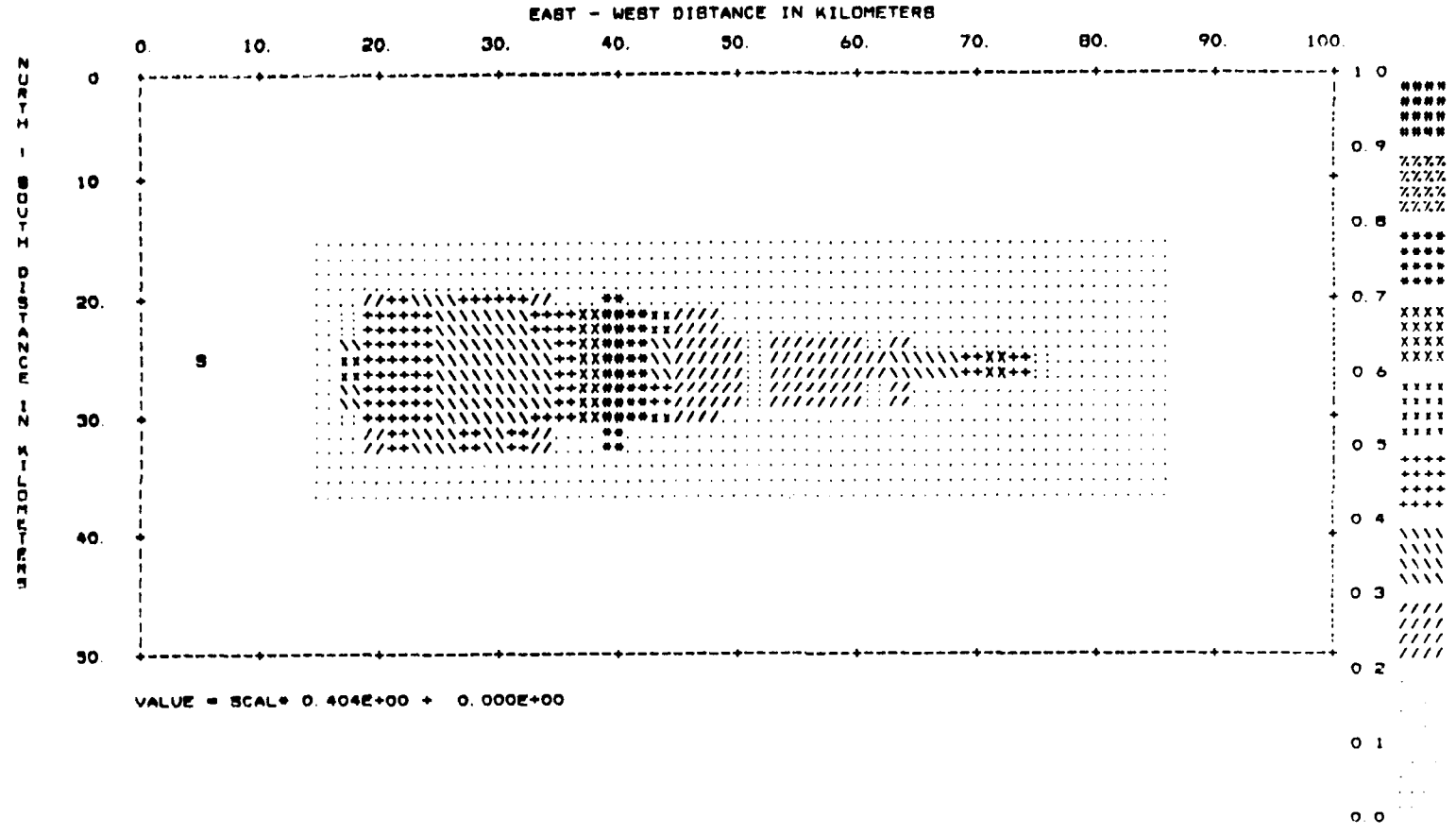
BASIN MODEL 2
PERIOD = 1.0000 SECONDS
EAST - WEST DISTANCE IN KILOMETERS
0.
10.
20.
30.
40.
50.
60.
70.
80.
90.
100.
NORTH - SOUTH DISTANCE IN KILOMETERS
0
10
20.
30.
40.
50.
S
1.0
0.9
0.8
0.7
0.6
0.5
0.4
0.3
0.2
0.1
0.0
VALUE = SCALE 0.404E+00 + 0.000E+00

FIGURE 16

BASIN 1. As before, sidewall effects are prominent when the source is more or less off to the side of the basin. The high intensities in Figure 10 can all be attributed to focusing of Type I and occasionally Type IV rays. Type I also dominates in Figure 11. Figures 12, 13, and 14 illustrate frequency dependent response (at 0.5, 2.0, and 16.0 hz) of the basin for a source off the narrow end. In these examples, Type I and IV rays cause the high amplitudes at the basin tip, Type I is responsible for the high intensity band at about 60 kilometers, and Type IV for the more distant (from the source) band at about 30 km. In Figure 15, Types I and IV rays are focused at the high amplitude area around 30 km; the more diffuse area of strong motion around 45 km are Type I rays only. Finally, in Figure 16 we plot the results for a source located off the wide end of the model. Here we again see a banded pattern with Type I rays causing the amplitudes at 45 km and Type IV producing the peak at the far end of the basin structure.

BASIN 3

Basin 3 is the tapered basin with the sloping basement contact. The results of the modeling studies with this structure are shown in Figures 17 through 27. Quite a lot of frequency dependence is apparent in these results. In the examples shown in Figures 17, 18, and 19 for the first source location and in Figure 20 for the second, Type I rays dominate at all of the frequencies and all regions of high amplitude. The increased localization of stronger intensities from the first source point is an interesting result for which an easy answer is not readily apparent. The frequency dependent shifts in Figures 21, 22, and 23 (at 1.0 hz, 4.0 hz, and 16.0 hz) are fairly subtle and may largely reflect numerical instabilities but are included here for completeness. Again, Types I and IV rays dominate a similar distribution to that observed for this source point and BASIN 2. In Figures 24, 25, and 26, frequency-dependent changes are readily apparent. Interestingly, almost all of the high amplitude regions reflect only Type I rays except for the very localized high at the center edge of the wide end of the basin. The last example for this basin is the

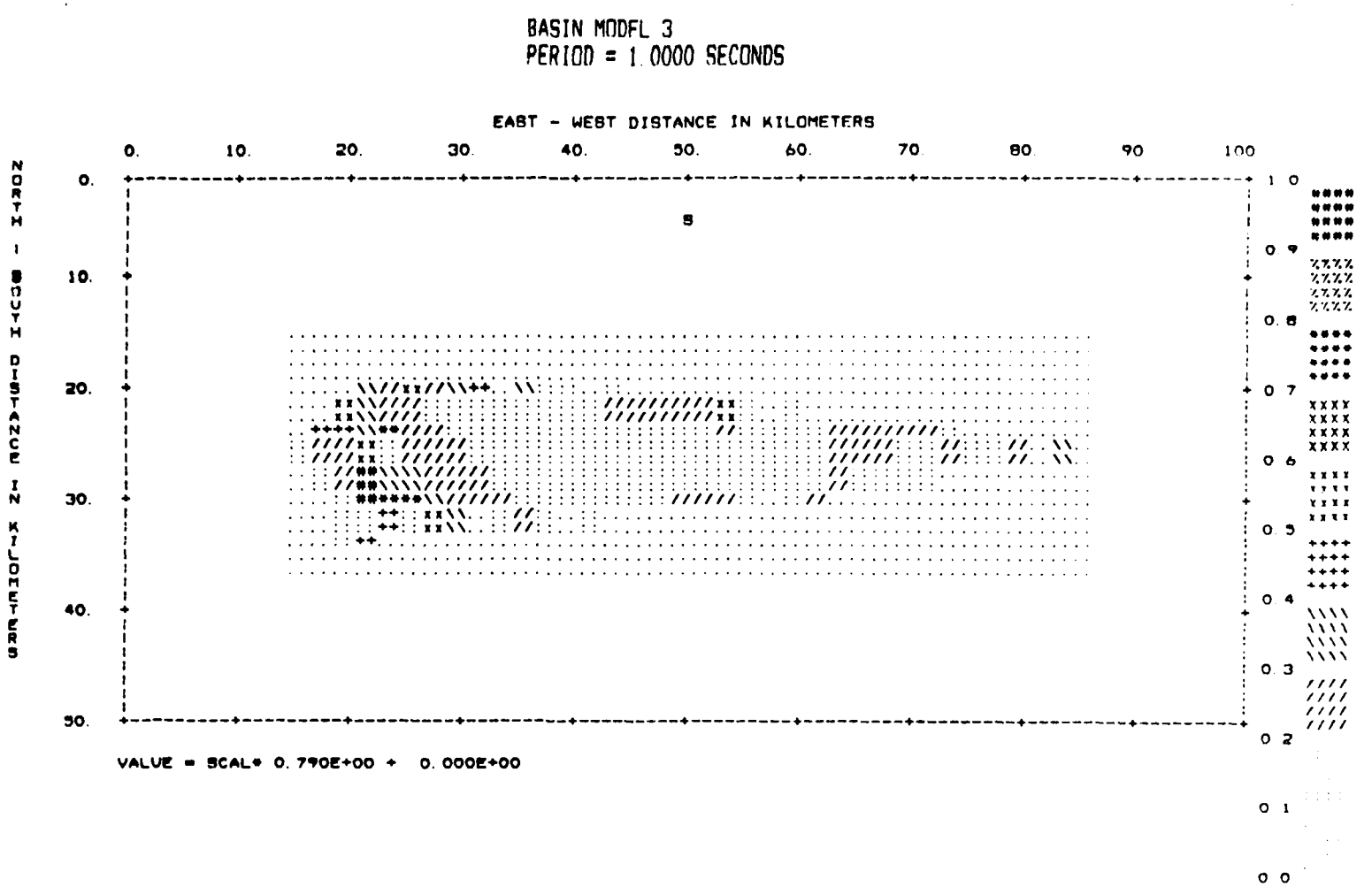
BASIN MODEL 3
PERIOD = 1.0000 SECONDS
EAST - WEST DISTANCE IN KILOMETERS
0. 10. 20. 30. 40. 50. 60. 70. 80. 90. 100.
NORTH - SOUTH DISTANCE IN KILOMETERS
0. 10. 20. 30. 40. 50.
S
1.0 0.9 0.8 0.7 0.6 0.5 0.4 0.3 0.2 0.1 0.0
VALUE = SCALE 0.790E+00 + 0.000E+00

FIGURE 17

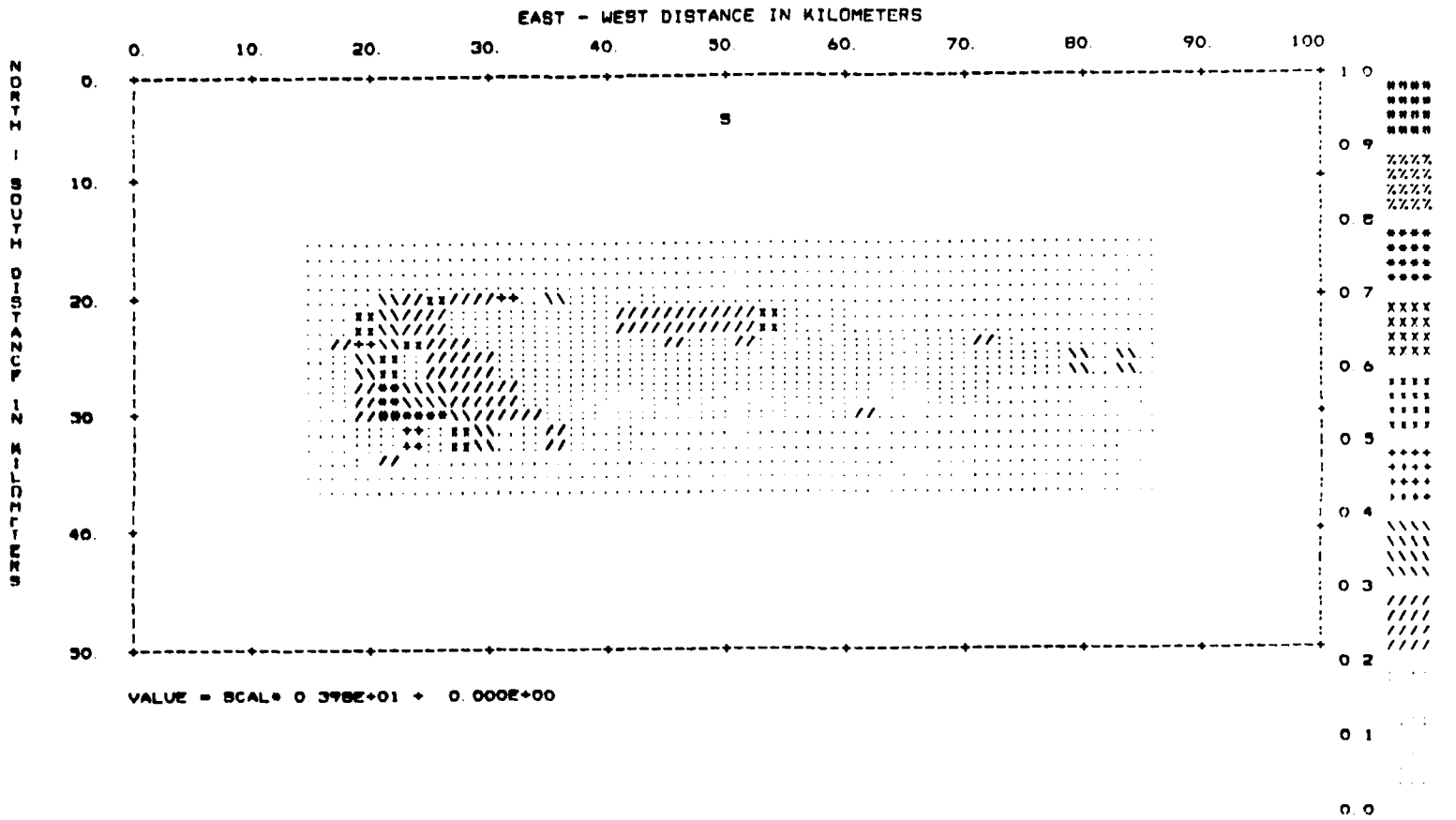
BASIN MODEL 3
PERIOD = 0.2500 SECONDS
EAST - WEST DISTANCE IN KILOMETERS
0. 10. 20. 30. 40. 50. 60. 70. 80. 90. 100
NORTH - SOUTH DISTANCE IN KILOMETERS
0. 10. 20. 30. 40. 50.
S
1.0 0.9 0.8 0.7 0.6 0.5 0.4 0.3 0.2 0.1 0.0
VALUE = SCALE 0.398E+01 + 0.000E+00

FIGURE 18

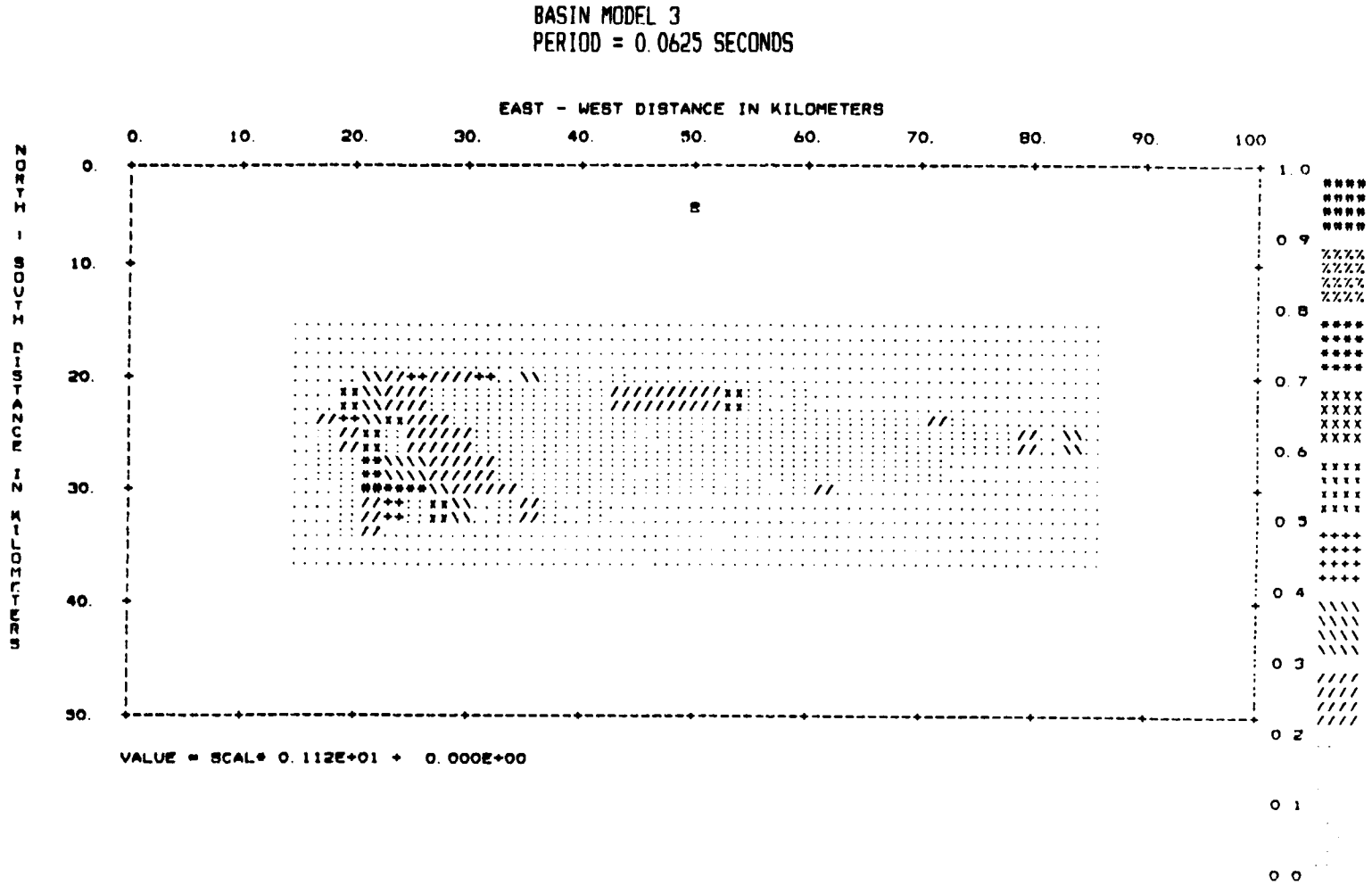
BASIN MODEL 3
PERIOD = 0.0625 SECONDS
EAST - WEST DISTANCE IN KILOMETERS
0. 10. 20. 30. 40. 50. 60. 70. 80. 90. 100
NORTH - SOUTH DISTANCE IN KILOMETERS
0. 10. 20. 30. 40. 50.
1.0 0.9 0.8 0.7 0.6 0.5 0.4 0.3 0.2 0.1 0.0
VALUE = SCALE 0.112E+01 + 0.000E+00

FIGURE 19

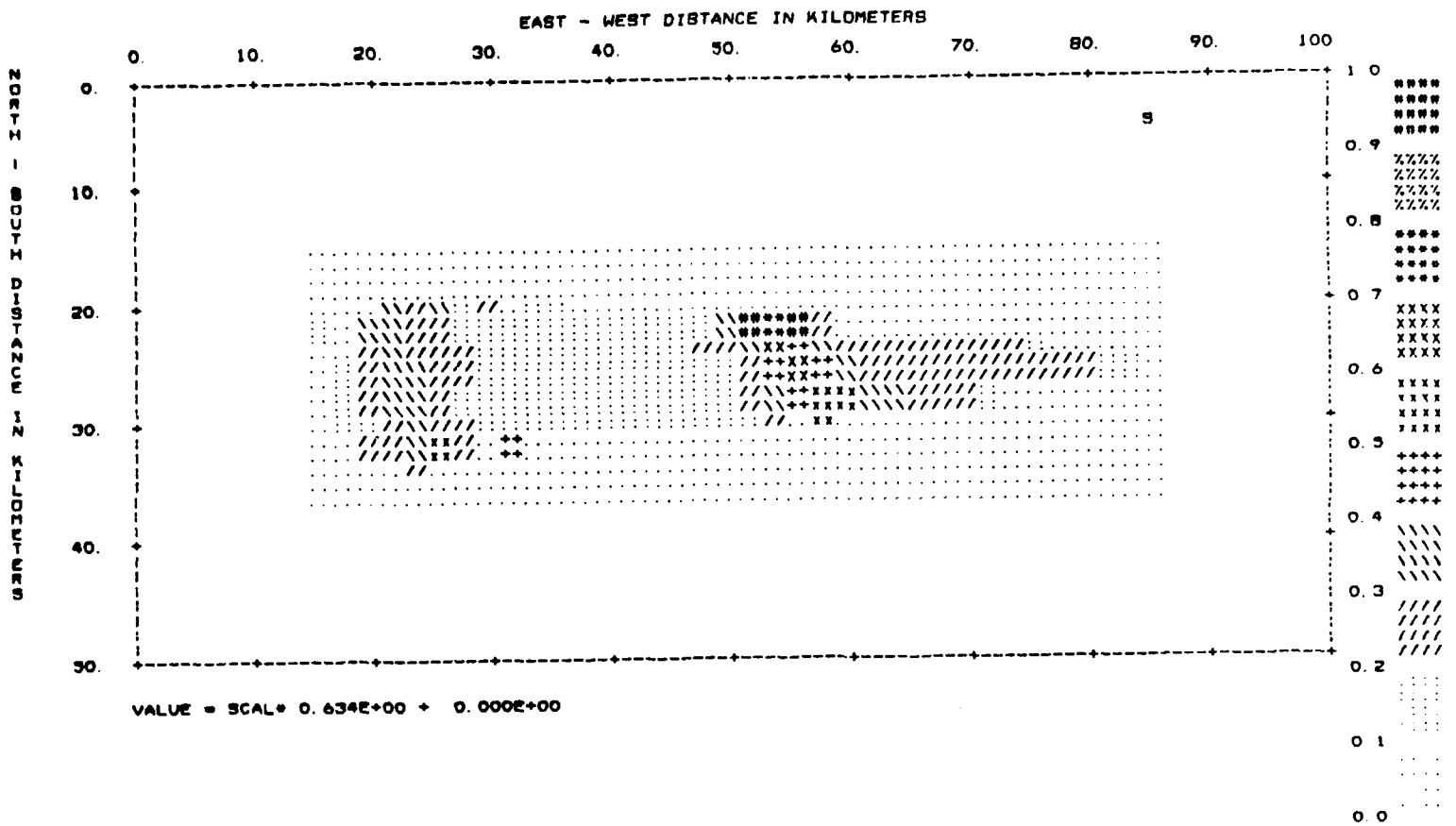
BASIN MODEL 3
PERIOD = 1.0000 SECONDS
EAST - WEST DISTANCE IN KILOMETERS
0.
10.
20.
30.
40.
50.
60.
70.
80.
90.
100
NORTH - SOUTH DISTANCE IN KILOMETERS
0.
10.
20.
30.
40.
50.
S
1.0
0.9
0.8
0.7
0.6
0.5
0.4
0.3
0.2
0.1
0.0
VALUE = SCALE 0.634E+00 + 0.000E+00

FIGURE 20

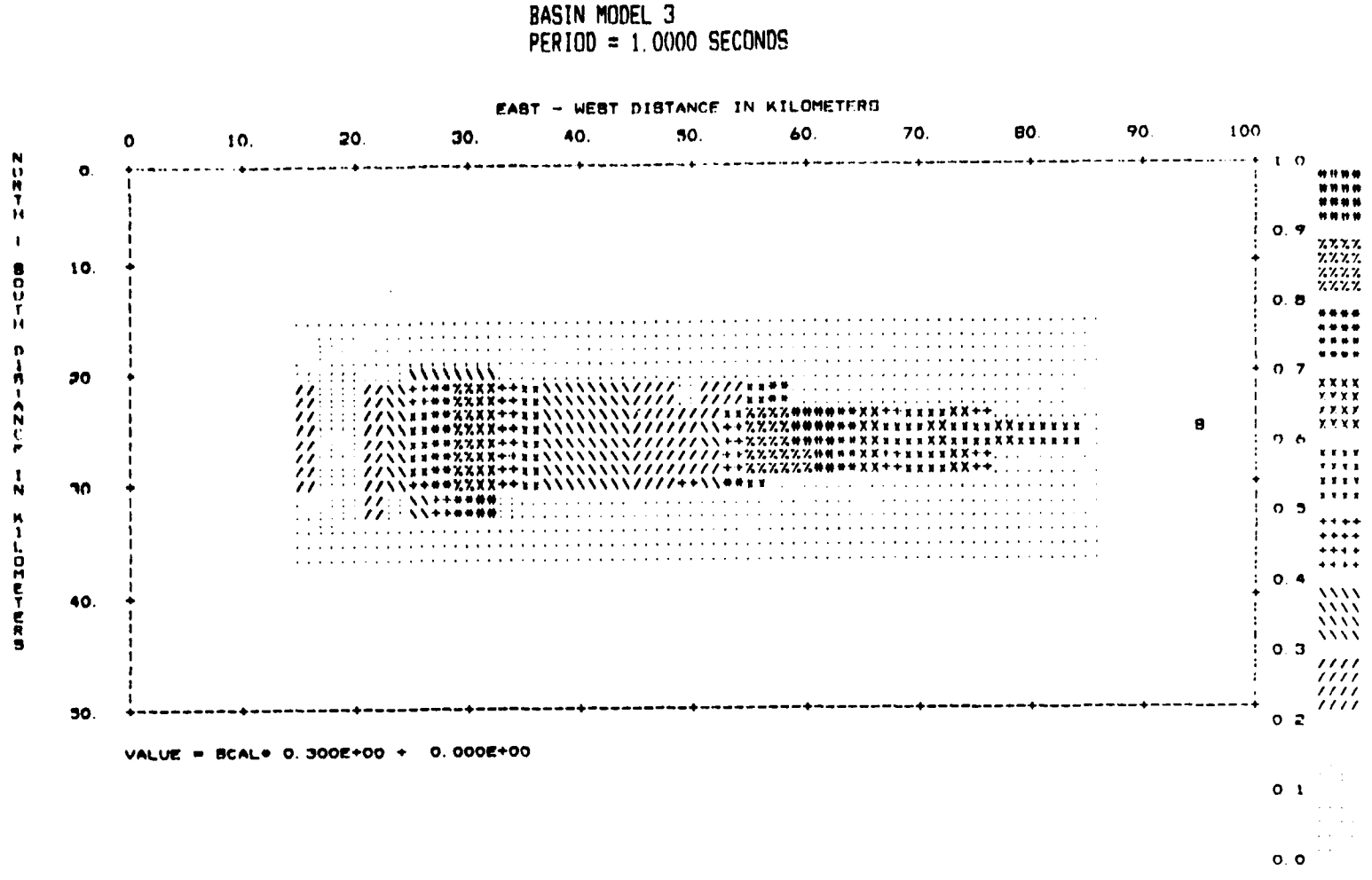
BASIN MODEL 3
PERIOD = 1.0000 SECONDS
EAST - WEST DISTANCE IN KILOMETERS
0
10.
20.
30.
40.
50.
60.
70.
80.
90.
100
NORTH - SOUTH DISTANCE IN KILOMETERS
0.
10.
20.
30.
40.
50.
1.0
0.9
0.8
0.7
0.6
0.5
0.4
0.3
0.2
0.1
0.0
VALUE = SCALE 0.300E+00 + 0.000E+00

FIGURE 21

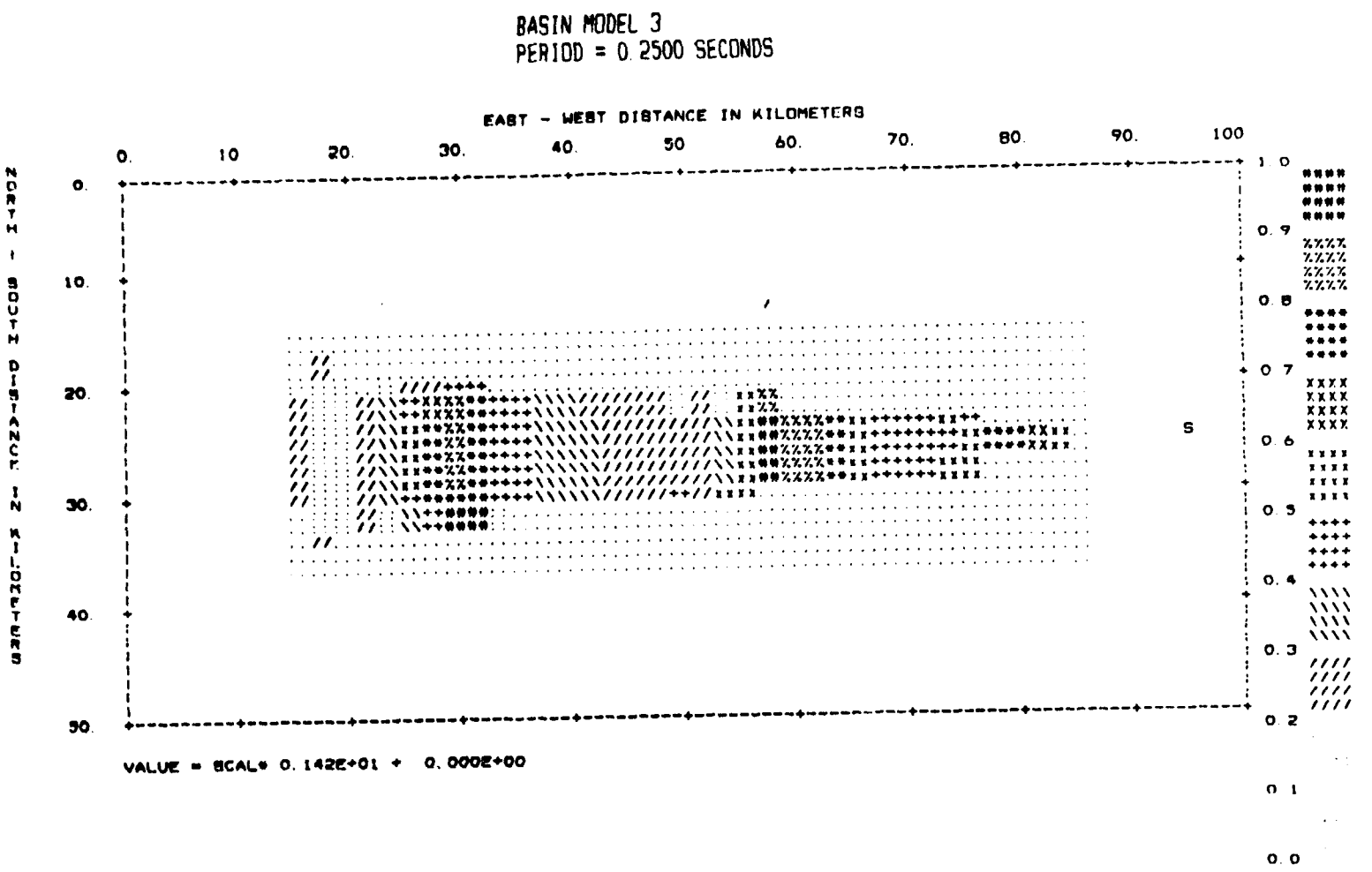
BASIN MODEL 3
PERIOD = 0.2500 SECONDS
EAST - WEST DISTANCE IN KILOMETERS
0.
10
20.
30.
40.
50
60.
70.
80.
90.
100
NORTH - SOUTH DISTANCE IN KILOMETERS
0.
10.
20.
30.
40.
50.
S
1.0
0.9
0.8
0.7
0.6
0.5
0.4
0.3
0.2
0.1
0.0
VALUE = SCALE 0.142E+01 + 0.000E+00

FIGURE 22

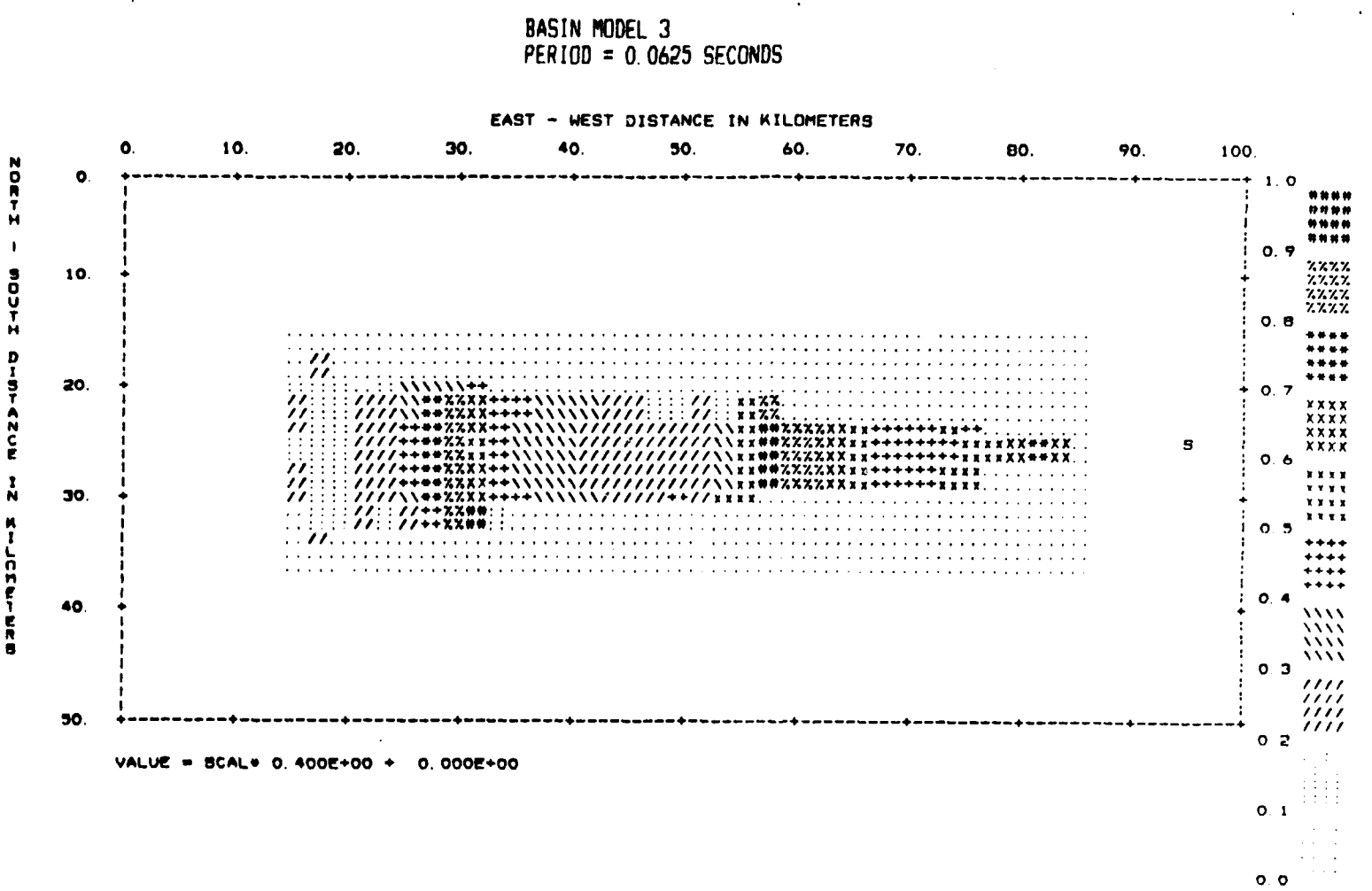
BASIN MODEL 3
PERIOD = 0.0625 SECONDS
EAST - WEST DISTANCE IN KILOMETERS
0. 10. 20. 30. 40. 50. 60. 70. 80. 90. 100.
NORTH - SOUTH DISTANCE IN KILOMETERS
0. 10. 20. 30. 40. 50.
S
1.0 0.9 0.8 0.7 0.6 0.5 0.4 0.3 0.2 0.1 0.0
VALUE = SCALE 0.400E+00 + 0.000E+00

FIGURE 23

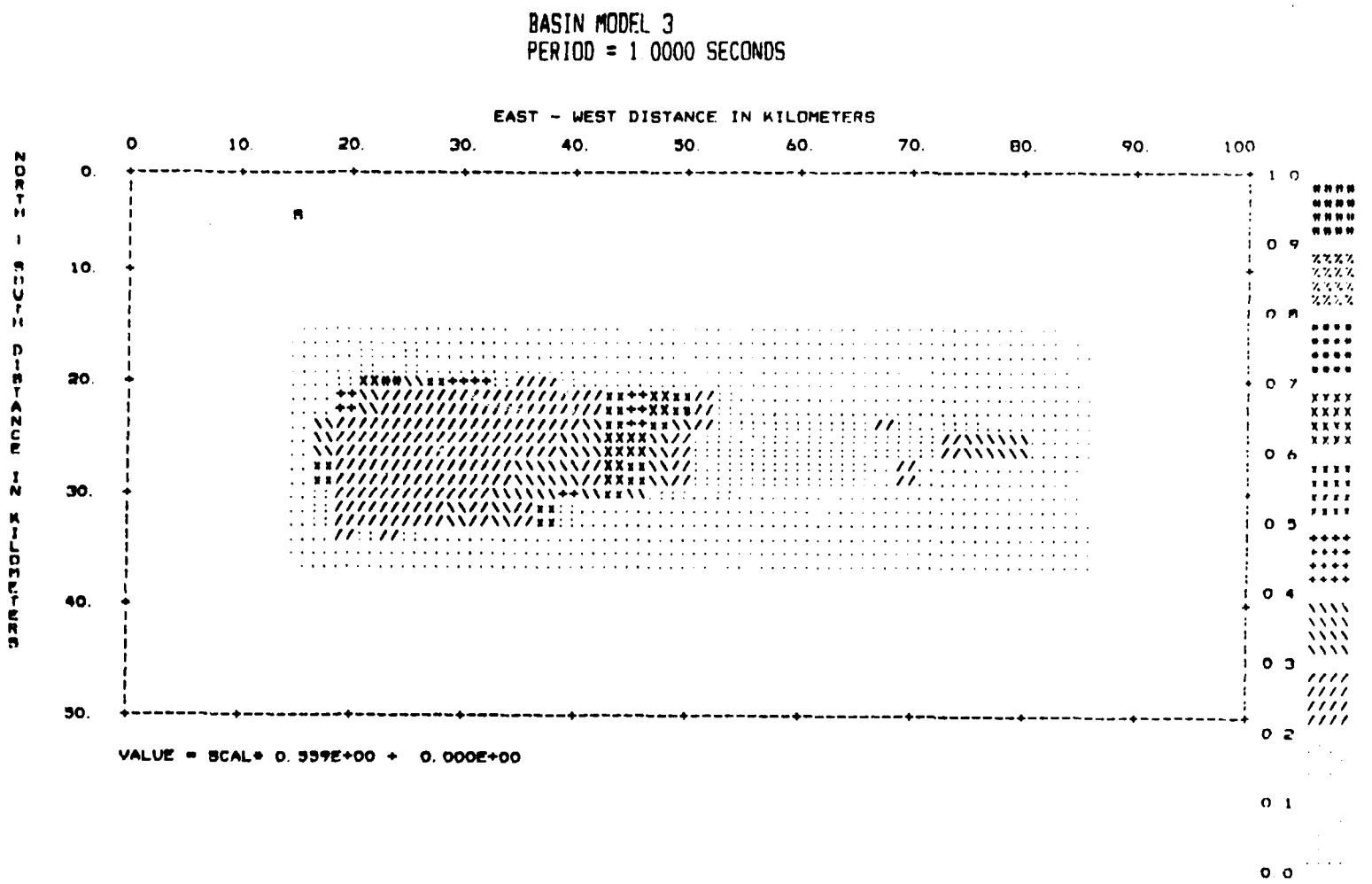
BASIN MODEL 3
PERIOD = 1 0000 SECONDS
EAST - WEST DISTANCE IN KILOMETERS
0
10.
20.
30.
40.
50.
60.
70.
80.
90.
100
NORTH - SOUTH DISTANCE IN KILOMETERS
0.
10.
20.
30.
40.
50.
1 0
0 9
0 8
0 7
0 6
0 5
0 4
0 3
0 2
0 1
0 0
VALUE = SCALE 0. 559E+00 + 0. 000E+00

FIGURE 24

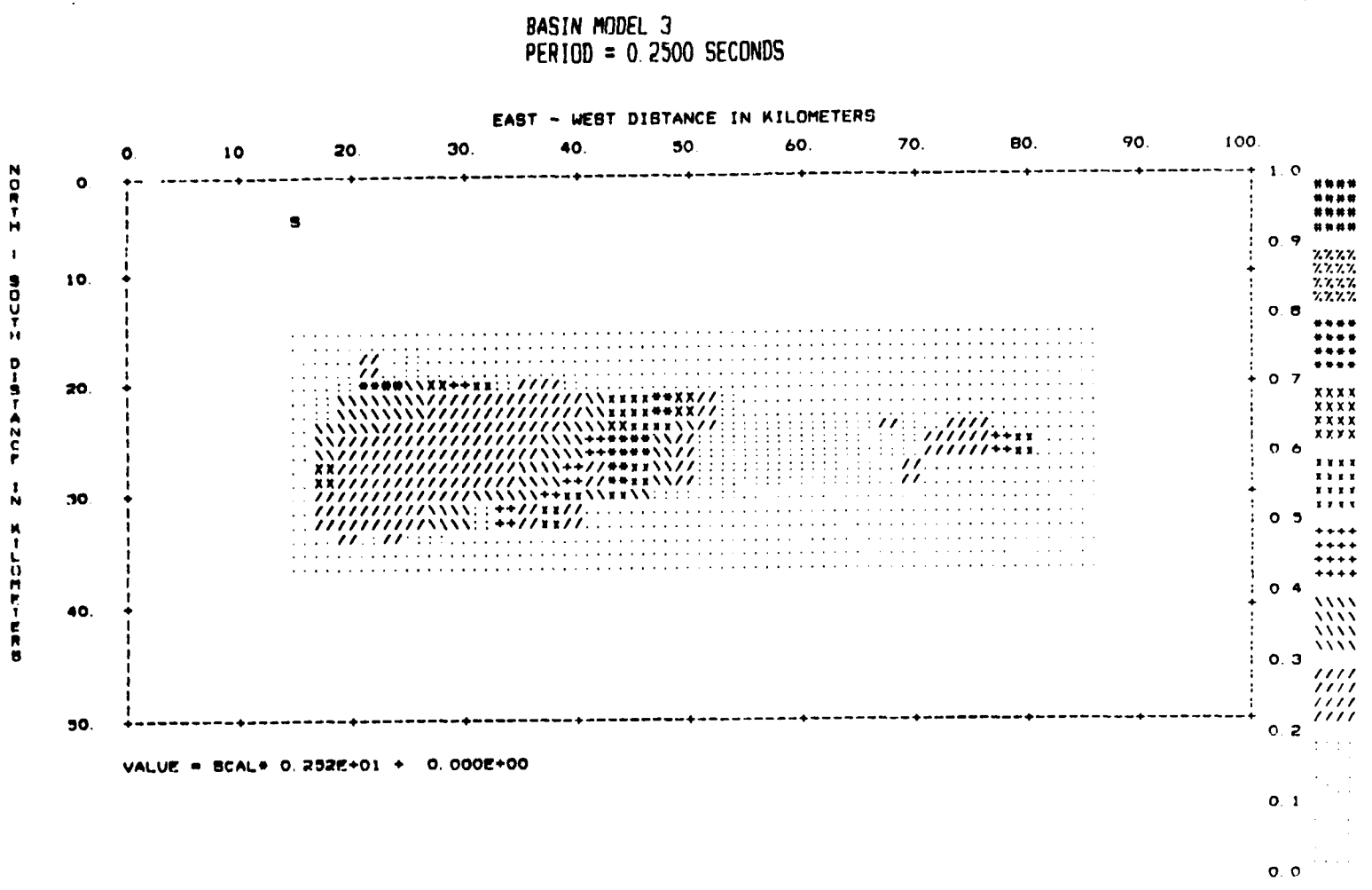
BASIN MODEL 3
PERIOD = 0.2500 SECONDS
EAST - WEST DISTANCE IN KILOMETERS
0.
10.
20.
30.
40.
50.
60.
70.
80.
90.
100.
NORTH - SOUTH DISTANCE IN KILOMETERS
0.
10.
20.
30.
40.
50.
1.0
0.9
0.8
0.7
0.6
0.5
0.4
0.3
0.2
0.1
0.0
S
VALUE = SCALE 0.252E+01 + 0.000E+00

FIGURE 25

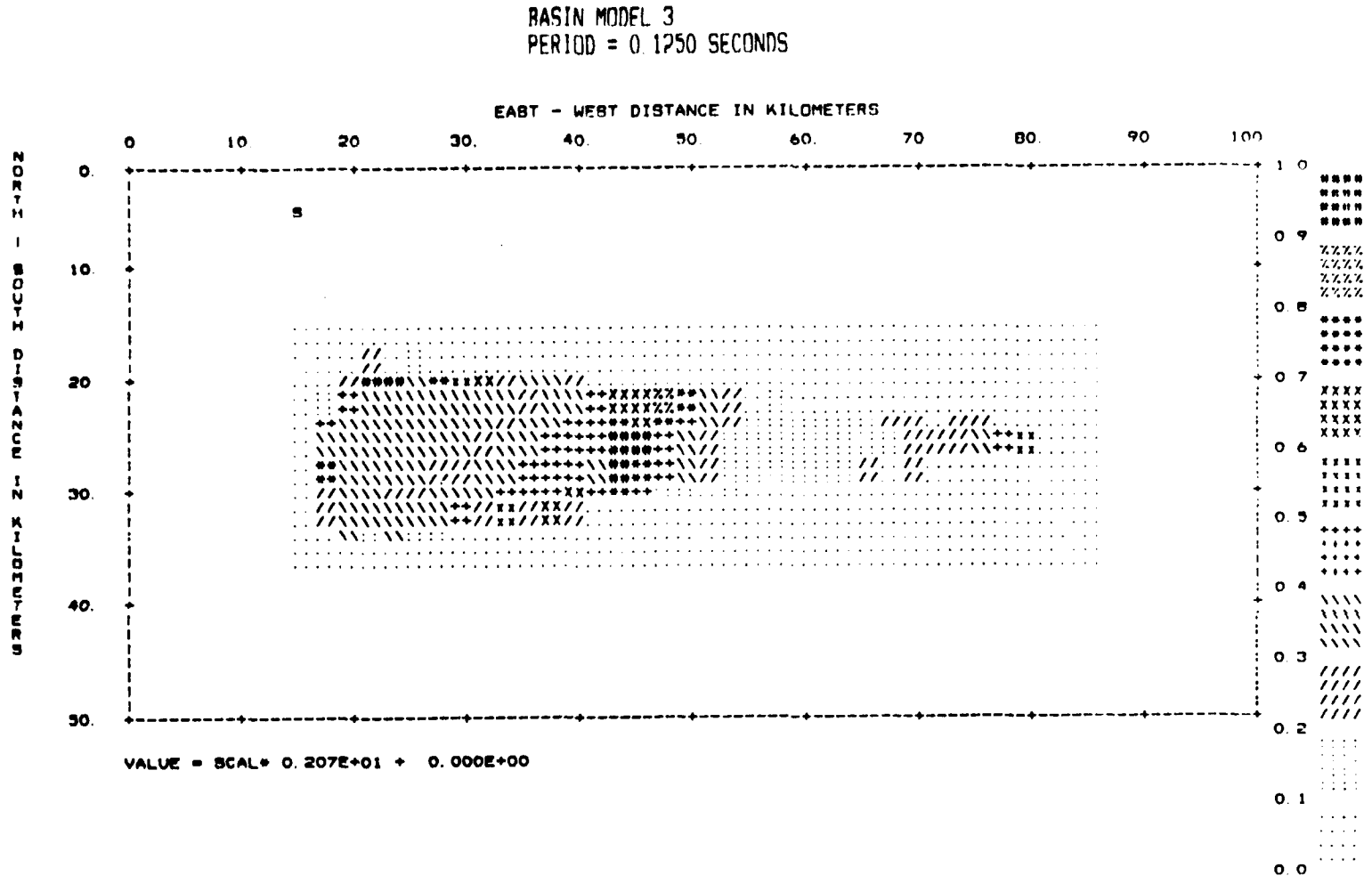
BASIN MODEL 3
PERIOD = 0.1250 SECONDS
EAST - WEST DISTANCE IN KILOMETERS
0
10
20
30.
40.
50.
60.
70
80.
90
100
NORTH - SOUTH DISTANCE IN KILOMETERS
0.
10.
20
30.
40.
50.
1.0
0.9
0.8
0.7
0.6
0.5
0.4
0.3
0.2
0.1
0.0
VALUE = SCALE 0.207E+01 + 0.000E+00

FIGURE 26

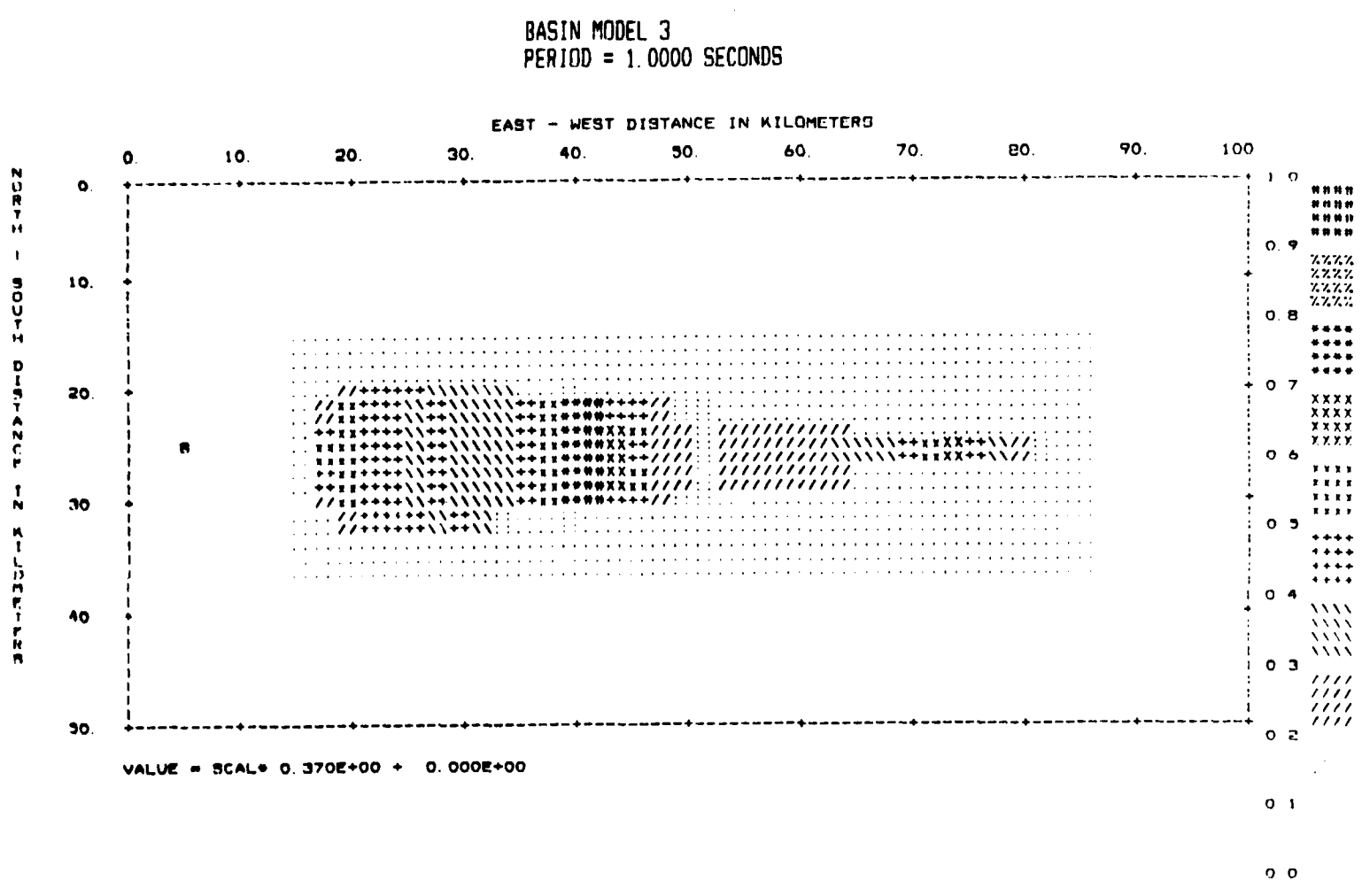
BASIN MODEL 3
PERIOD = 1.0000 SECONDS
EAST - WEST DISTANCE IN KILOMETERS
0. 10. 20. 30. 40. 50. 60. 70. 80. 90. 100
NORTH - SOUTH DISTANCE IN KILOMETERS
0. 10. 20. 30. 40. 50.
1.0 0.9 0.8 0.7 0.6 0.5 0.4 0.3 0.2 0.1 0.0
VALUE = SCALE 0.370E+00 + 0.000E+00

FIGURE 27

most interesting of all the models examined through this phase of the project. While no particular frequency dependence is apparent here, this is the only example found in which multiples, specifically rays of Types V and VI were substantial contributors to the areas of highest intensity. In this example, Type I rays dominate the high central band regions and Type IV rays produce the high amplitudes and the wide end of the basin. The strong motion predicted toward the narrow end of the basin, however, is the result of constructive interference of Types IV, V and VI rays.

BASIN 4

Figures 28 through 40 illustrate the results of models of the asymmetric basin model. It is with this rather more complicated model that we see the most frequency-dependent phenomena. Almost all of the strong amplitudes in these examples are the result of Type I ray focusing. Only in Figures 34, 37, and 38 which display the results of models for sources either directly off the long axis of the basin (Fig. 34 and 38) or slightly offset to the south of the wide end of the basin (Fig. 37) are type IV rays important. In Figures 34 and 38, Type IV rays are substantial contributors to the nearest and farthest (from the source) regions of high intensity but not to the center bands. In Figure 37, Type IV rays are contributors only to the close-in (to the source) peak. Far more striking, however, are the fairly dramatic frequency-dependent shifts observed in these examples. We do not as yet understand why such effects should be more prominent in this particular model. The observation is largely the impetus behind the Gaussian beam methodology development to help confirm these results.

BASIN 5

BASIN 5 is a modification of the symmetric model used for BASIN 1. Here the basin sidewalls dip at 30° instead of 60°. The results of the modeling of this last basin in the series are illustrated in Figures 41

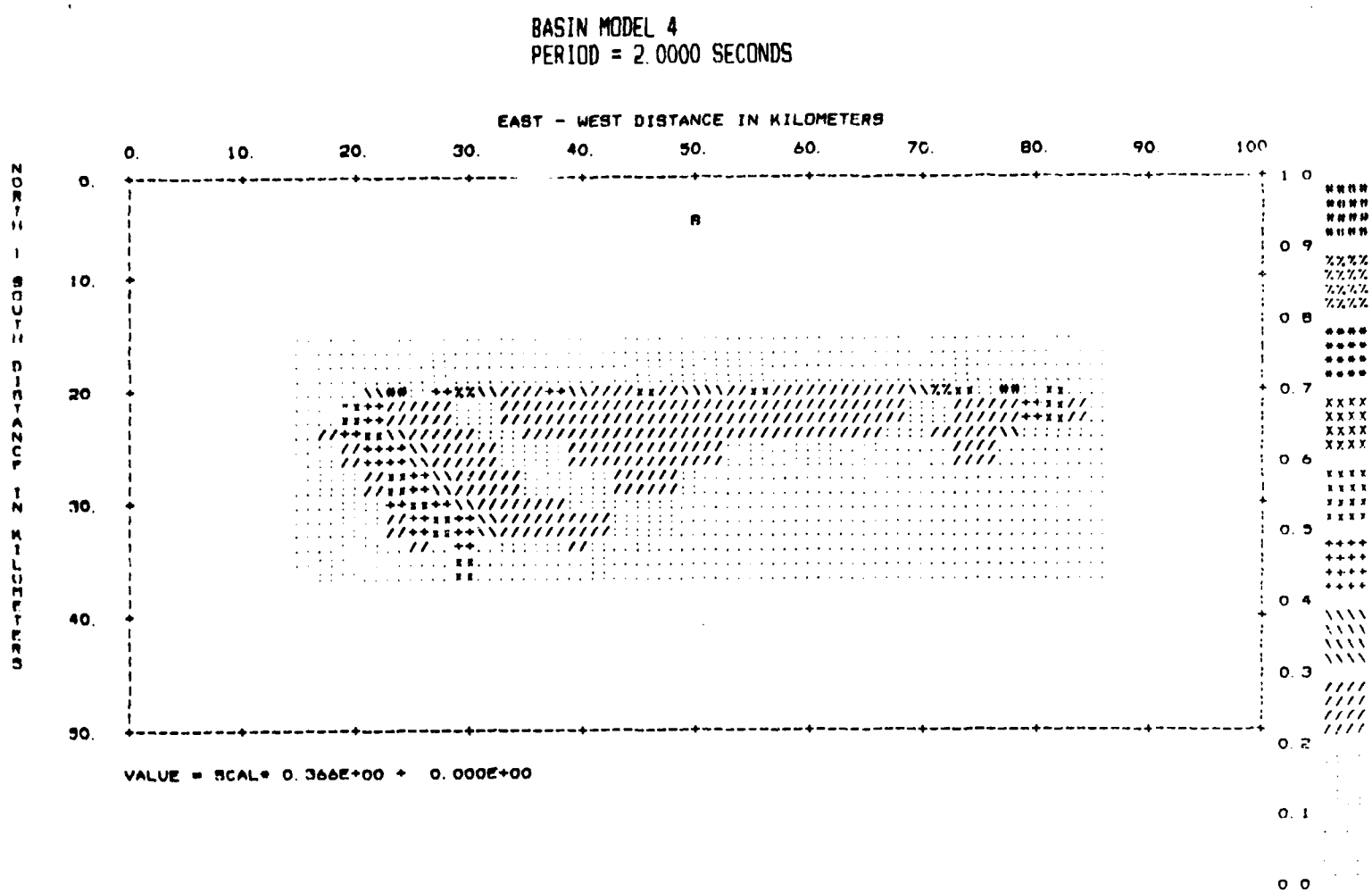
BASIN MODEL 4
PERIOD = 2.0000 SECONDS
EAST - WEST DISTANCE IN KILOMETERS
0. 10. 20. 30. 40. 50. 60. 70. 80. 90. 100
NORTH - SOUTH DISTANCE IN KILOMETERS
0. 10. 20. 30. 40. 50.
1.0 0.9 0.8 0.7 0.6 0.5 0.4 0.3 0.2 0.1 0.0
VALUE = SCALE 0.366E+00 + 0.000E+00

FIGURE 28

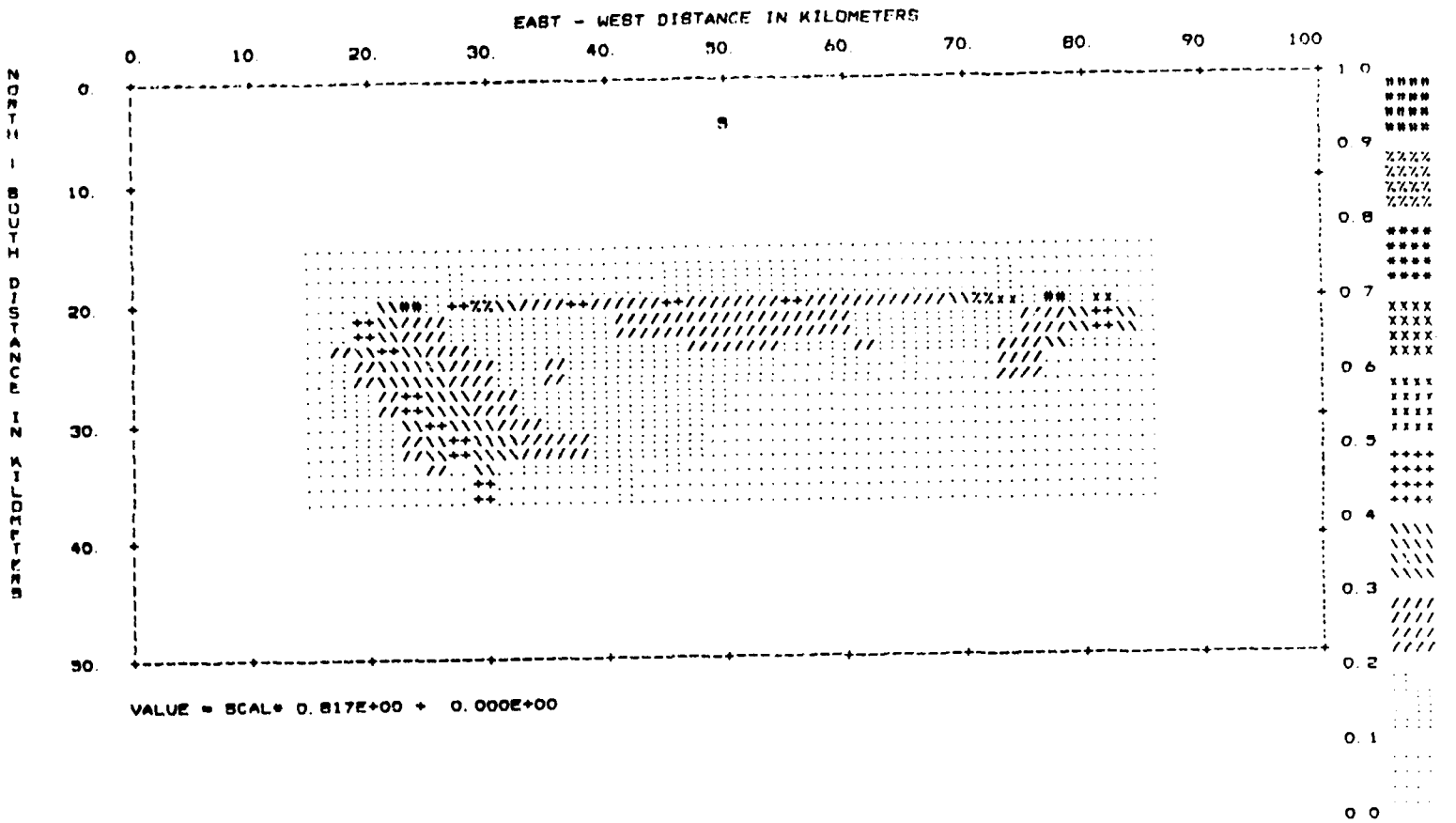
BASIN MODEL 4
PERIOD = 1.0000 SECONDS
EAST - WEST DISTANCE IN KILOMETERS
0. 10. 20. 30. 40. 50. 60. 70. 80. 90 100
NORTH - SOUTH DISTANCE IN KILOMETERS
0. 10. 20. 30. 40. 50.
1.0 0.9 0.8 0.7 0.6 0.5 0.4 0.3 0.2 0.1 0.0
VALUE = SCALE 0.817E+00 + 0.000E+00

FIGURE 29

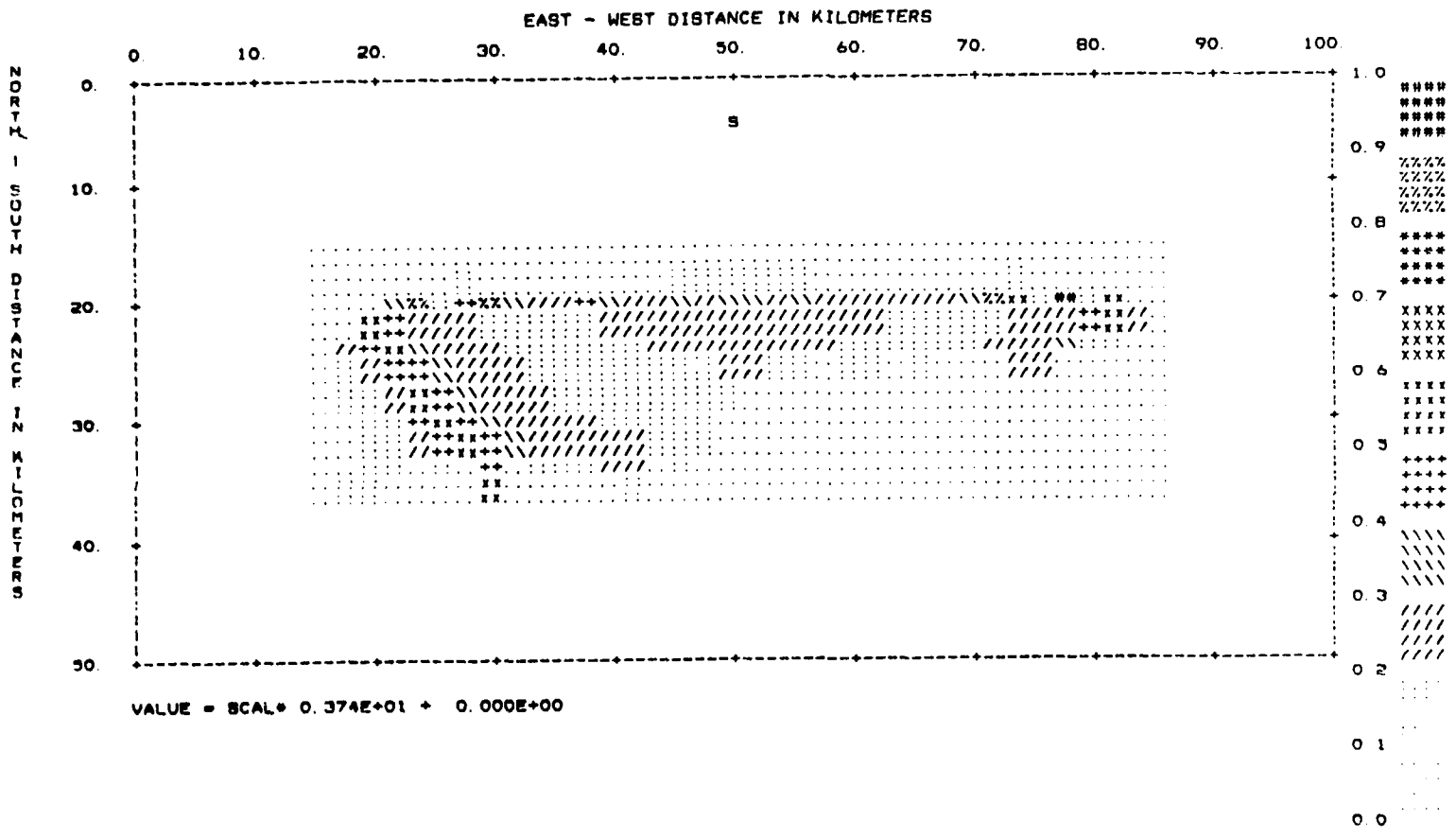
BASIN MODEL 4
PERIOD = 0.2500 SECONDS
EAST - WEST DISTANCE IN KILOMETERS
0
10.
20.
30.
40.
50.
60.
70.
80.
90.
100
NORTH - SOUTH DISTANCE IN KILOMETERS
0.
10.
20.
30.
40.
50.
S
1.0
0.9
0.8
0.7
0.6
0.5
0.4
0.3
0.2
0.1
0.0
VALUE = SCALE 0.374E+01 + 0.000E+00

FIGURE 30

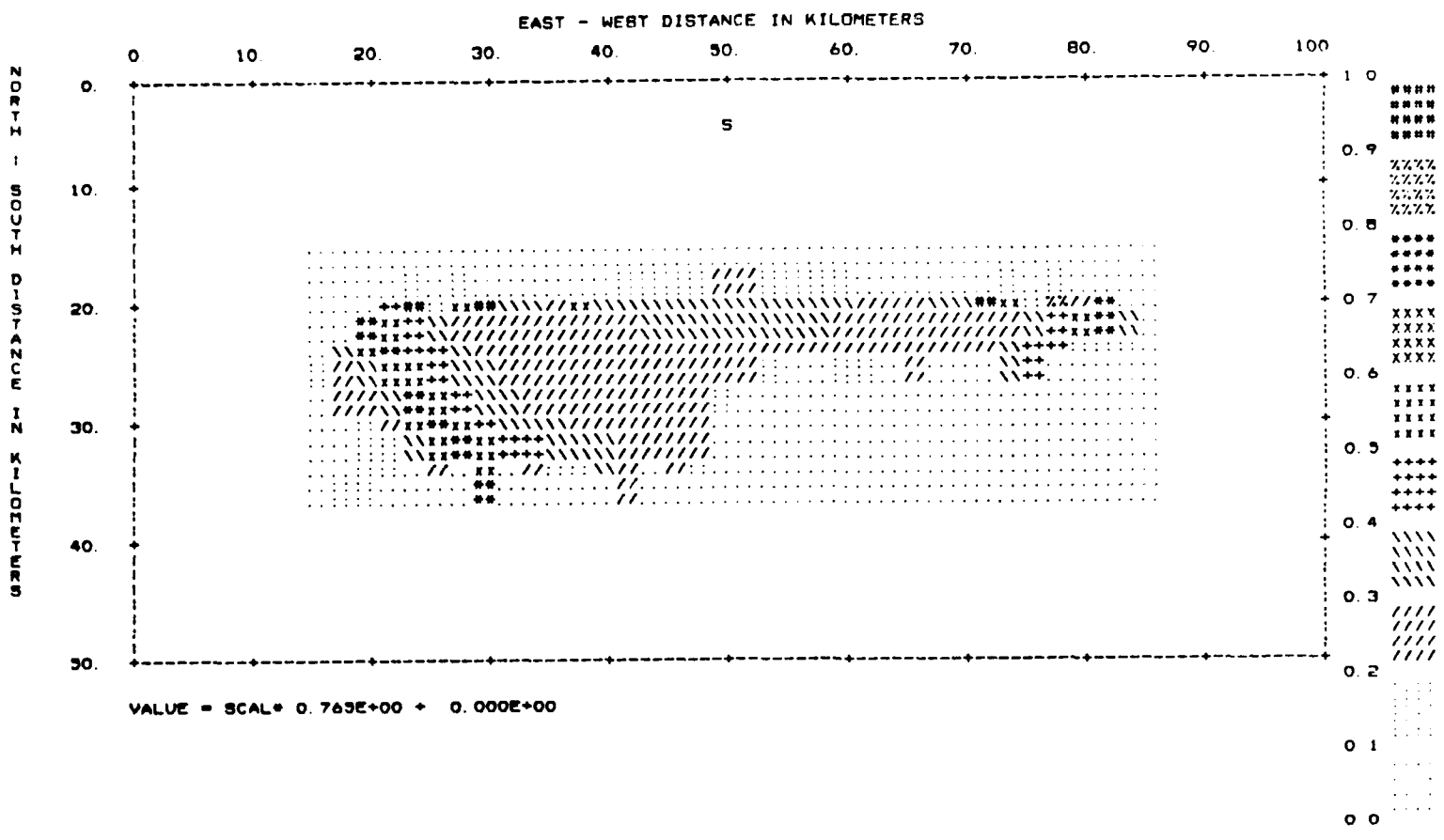
BASIN MODEL 4
PERIOD = 0 0625 SECONDS
EAST - WEST DISTANCE IN KILOMETERS
0
10.
20.
30.
40.
50.
60.
70.
80.
90.
100
NORTH - SOUTH DISTANCE IN KILOMETERS
0.
10.
20.
30.
40.
50.
S
1 0
0 9
0 8
0 7
0 6
0 5
0 4
0 3
0 2
0 1
0 0
VALUE = SCALE 0 769E+00 + 0 000E+00

FIGURE 31

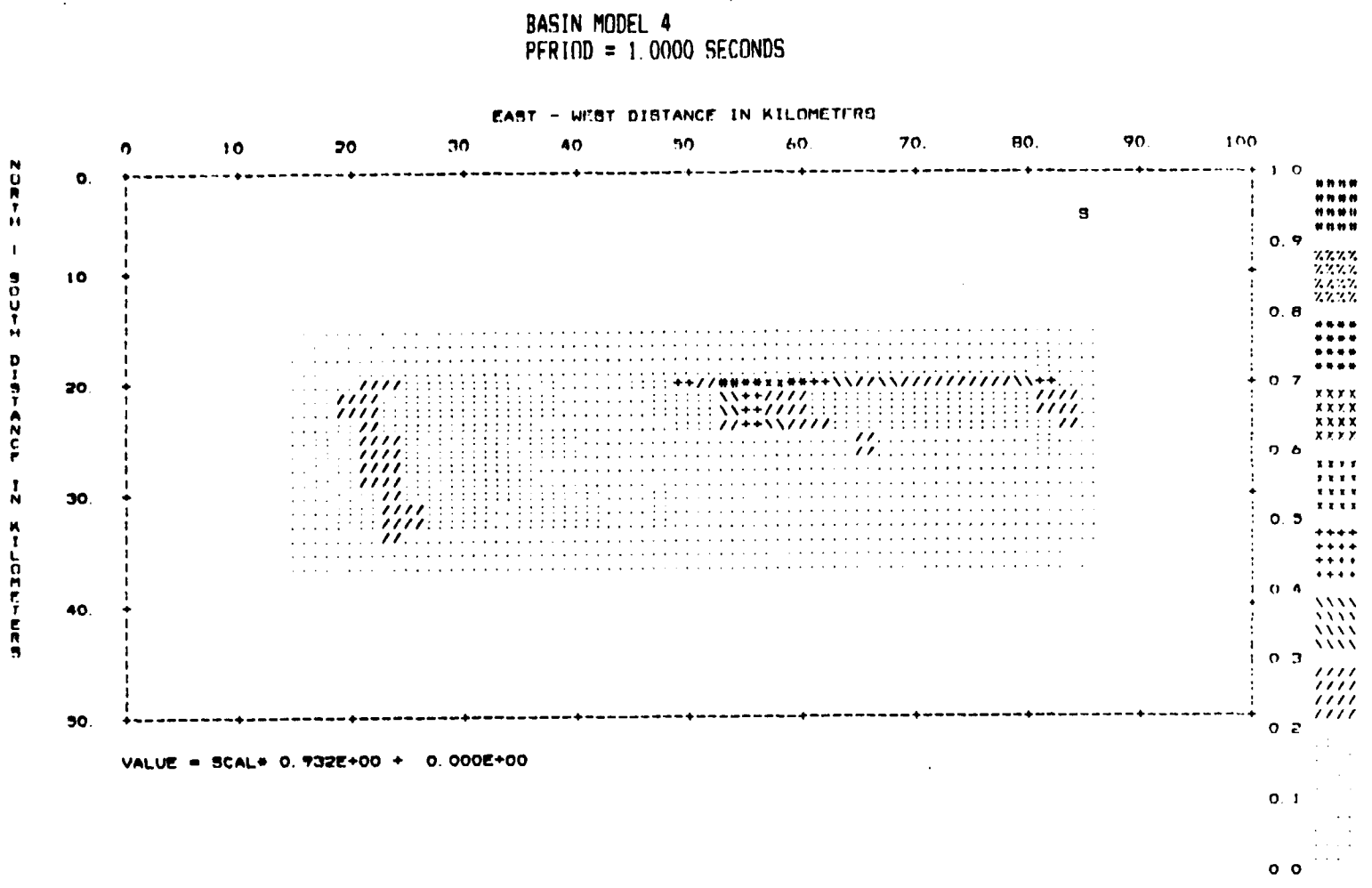
BASIN MODEL 4
PERIOD = 1.0000 SECONDS
EAST - WEST DISTANCE IN KILOMETERS
0
10
20
30
40
50
60
70.
80.
90.
100
NORTH - SOUTH DISTANCE IN KILOMETERS
0.
10
20.
30.
40.
50.
S
1.0
0.9
0.8
0.7
0.6
0.5
0.4
0.3
0.2
0.1
0.0
VALUE = SCALE 0.732E+00 + 0.000E+00

FIGURE 32

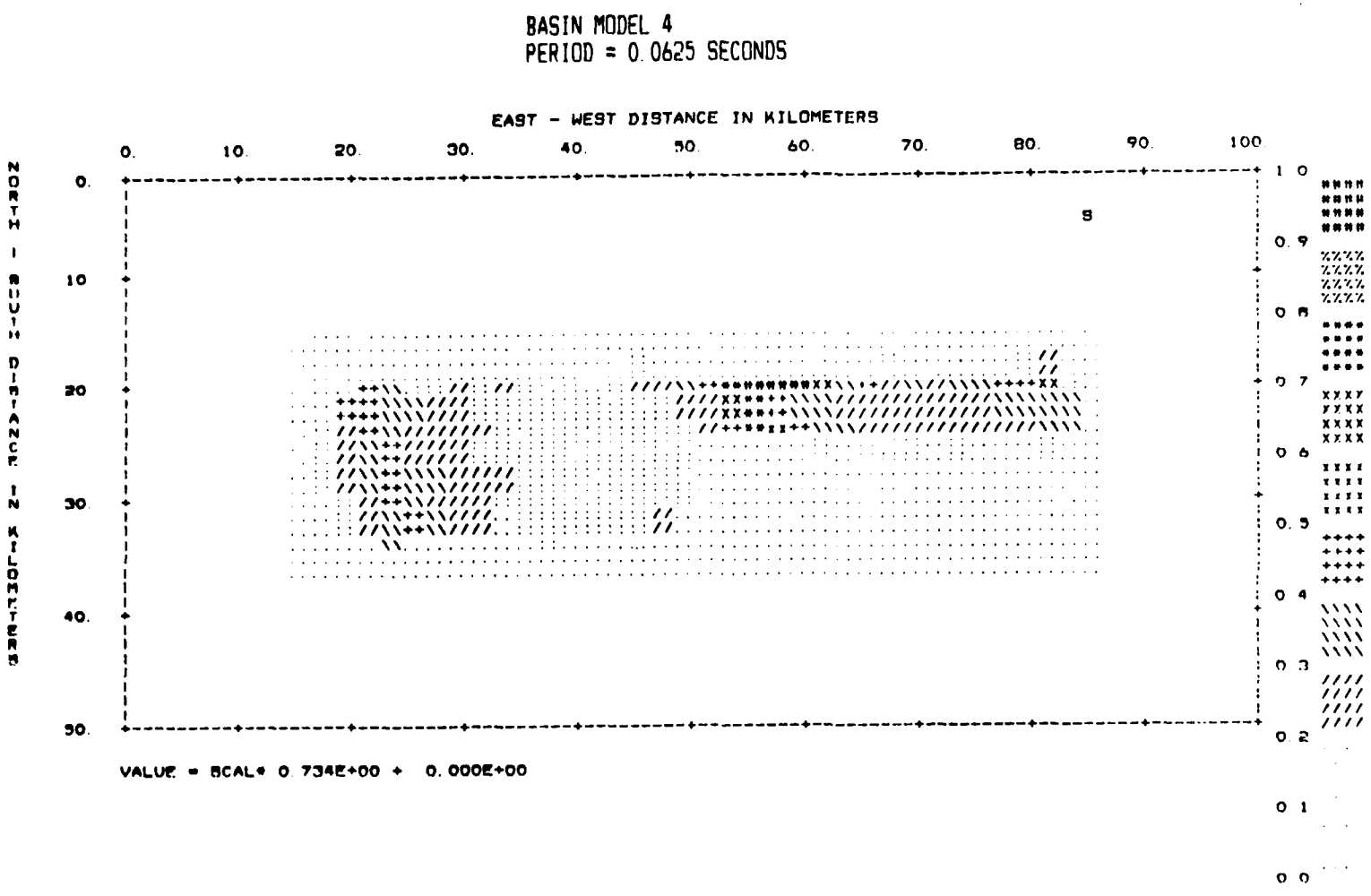
BASIN MODEL 4
PERIOD = 0.0625 SECONDS
EAST - WEST DISTANCE IN KILOMETERS
0. 10. 20. 30. 40. 50. 60. 70. 80. 90. 100
NORTH - SOUTH DISTANCE IN KILOMETERS
0. 10. 20. 30. 40. 50.
S
1.0 0.9 0.8 0.7 0.6 0.5 0.4 0.3 0.2 0.1 0.0
VALUE = SCALE 0.734E+00 + 0.000E+00

FIGURE 33

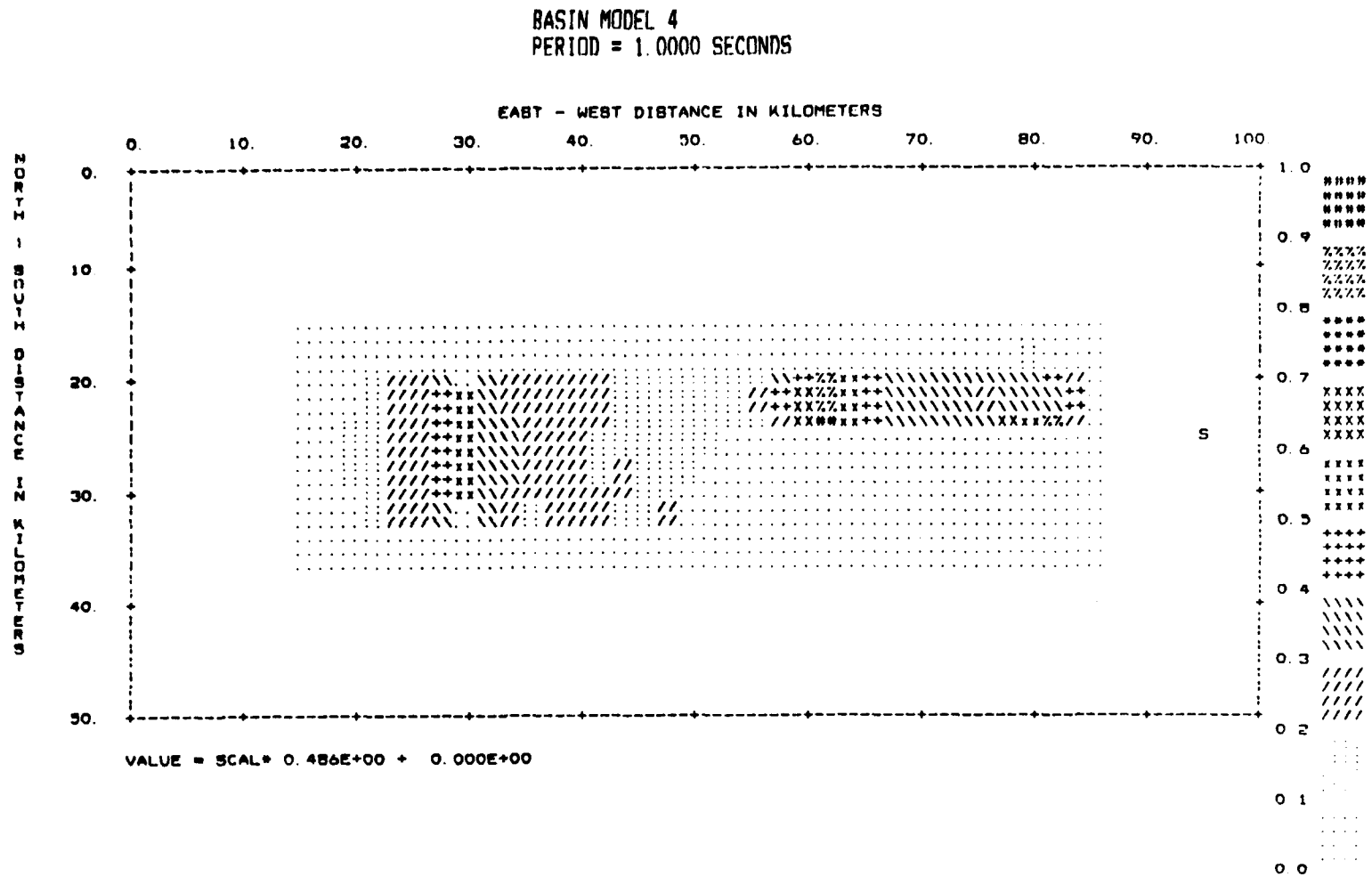
BASIN MODEL 4
PERIOD = 1.0000 SECONDS
EAST - WEST DISTANCE IN KILOMETERS
0.
10.
20.
30.
40.
50.
60.
70.
80.
90.
100
NORTH - SOUTH DISTANCE IN KILOMETERS
0.
10
20.
30.
40.
50.
S
1.0
0.9
0.8
0.7
0.6
0.5
0.4
0.3
0.2
0.1
0.0
VALUE = SCALE 0.486E+00 + 0.000E+00

FIGURE 34

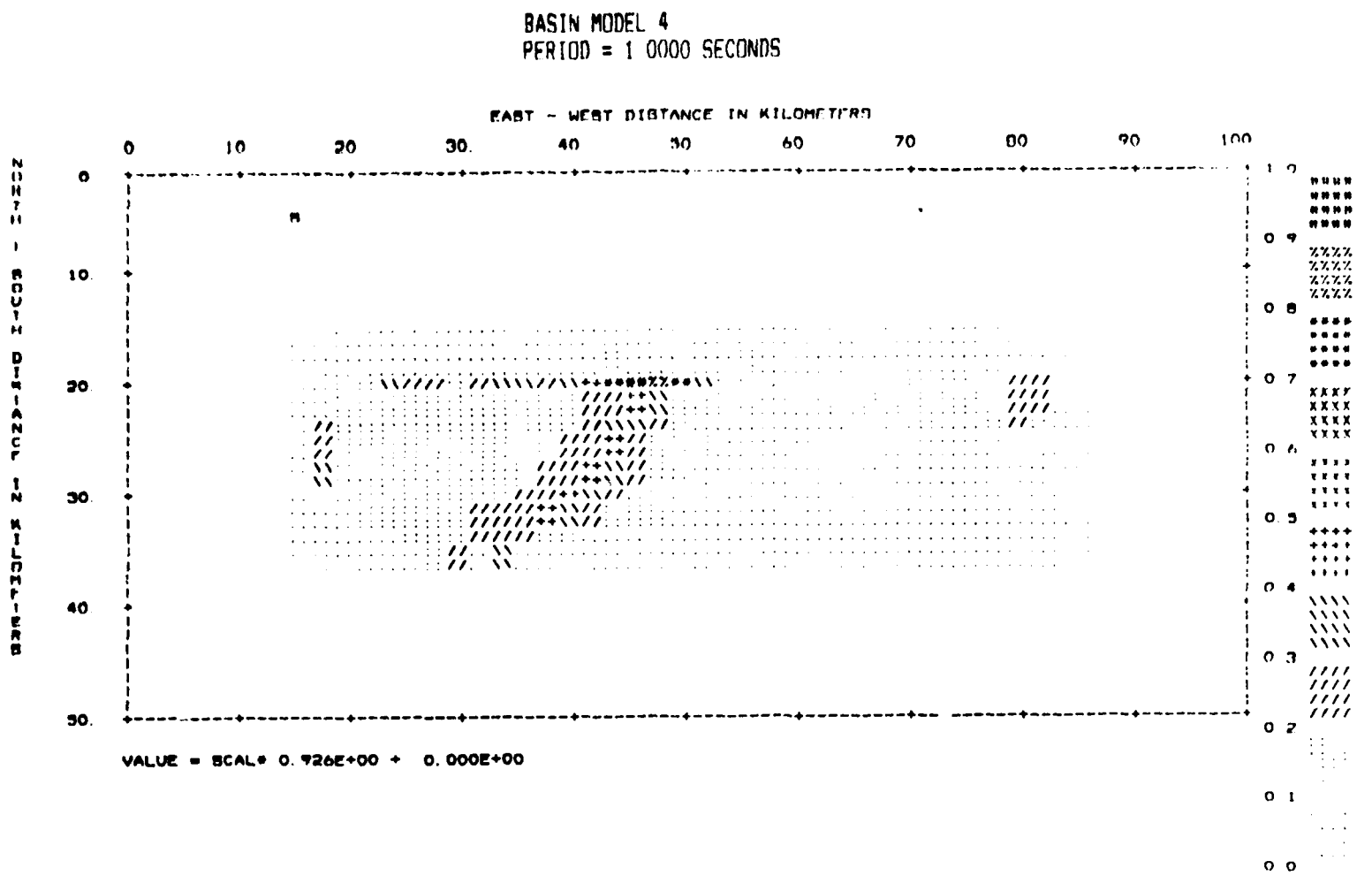
BASIN MODEL 4
PERIOD = 1 0000 SECONDS
EAST - WEST DISTANCE IN KILOMETERS
0
10
20
30
40
50
60
70
80
90
100
NORTH - SOUTH DISTANCE IN KILOMETERS
0
10
20
30
40
50
VALUE = SCALE 0.726E+00 + 0.000E+00
1.0
0.9
0.8
0.7
0.6
0.5
0.4
0.3
0.2
0.1
0.0

FIGURE 35

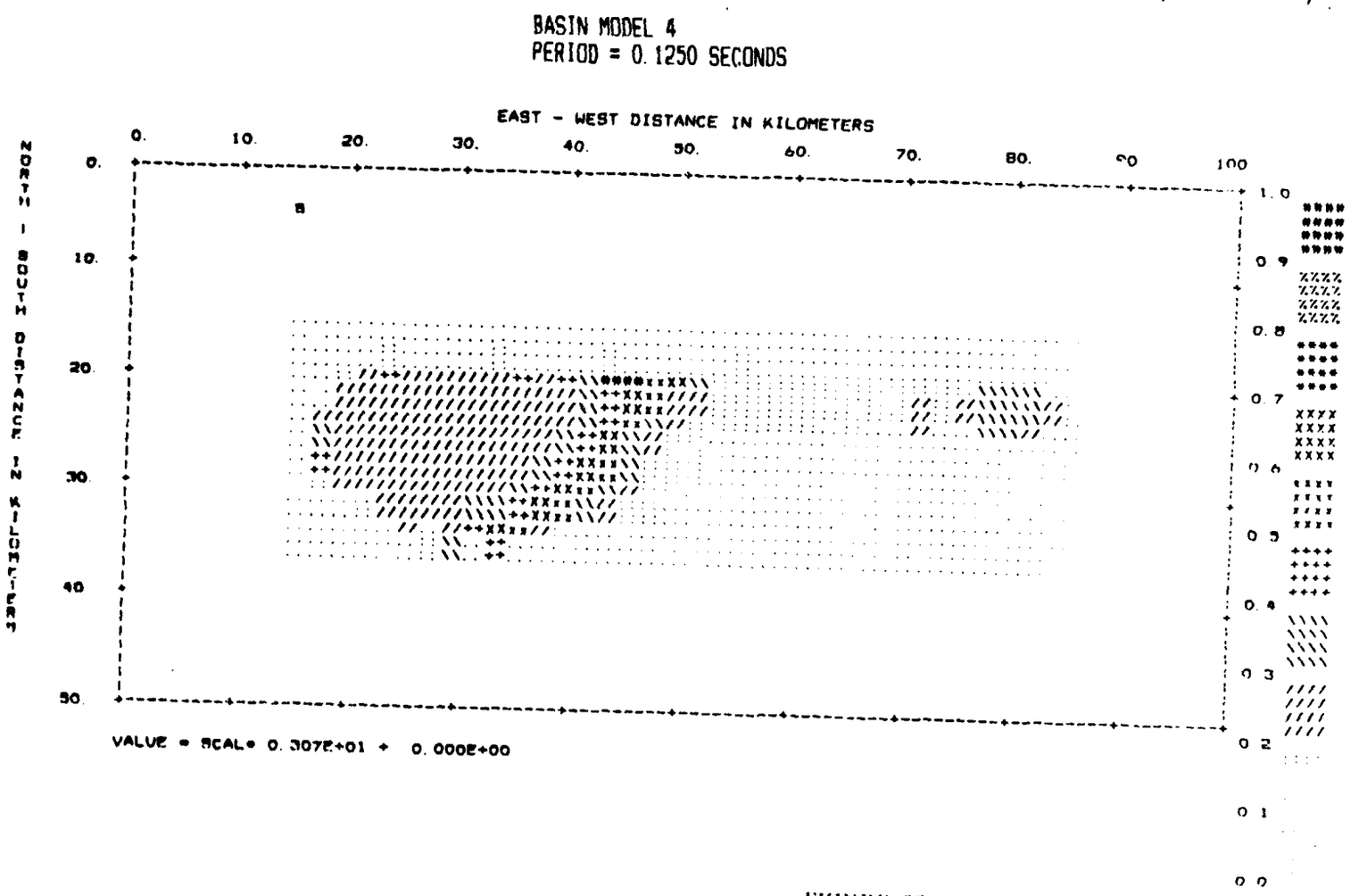
BASIN MODEL 4
PERIOD = 0.1250 SECONDS
EAST - WEST DISTANCE IN KILOMETERS
0.
10.
20.
30.
40.
50.
60.
70.
80.
90
100
NORTH - SOUTH DISTANCE IN KILOMETERS
0.
10.
20.
30.
40.
50.
B
1.0
0.9
0.8
0.7
0.6
0.5
0.4
0.3
0.2
0.1
0.0
VALUE = SCALE 0.307E+01 + 0.000E+00

FIGURE 36

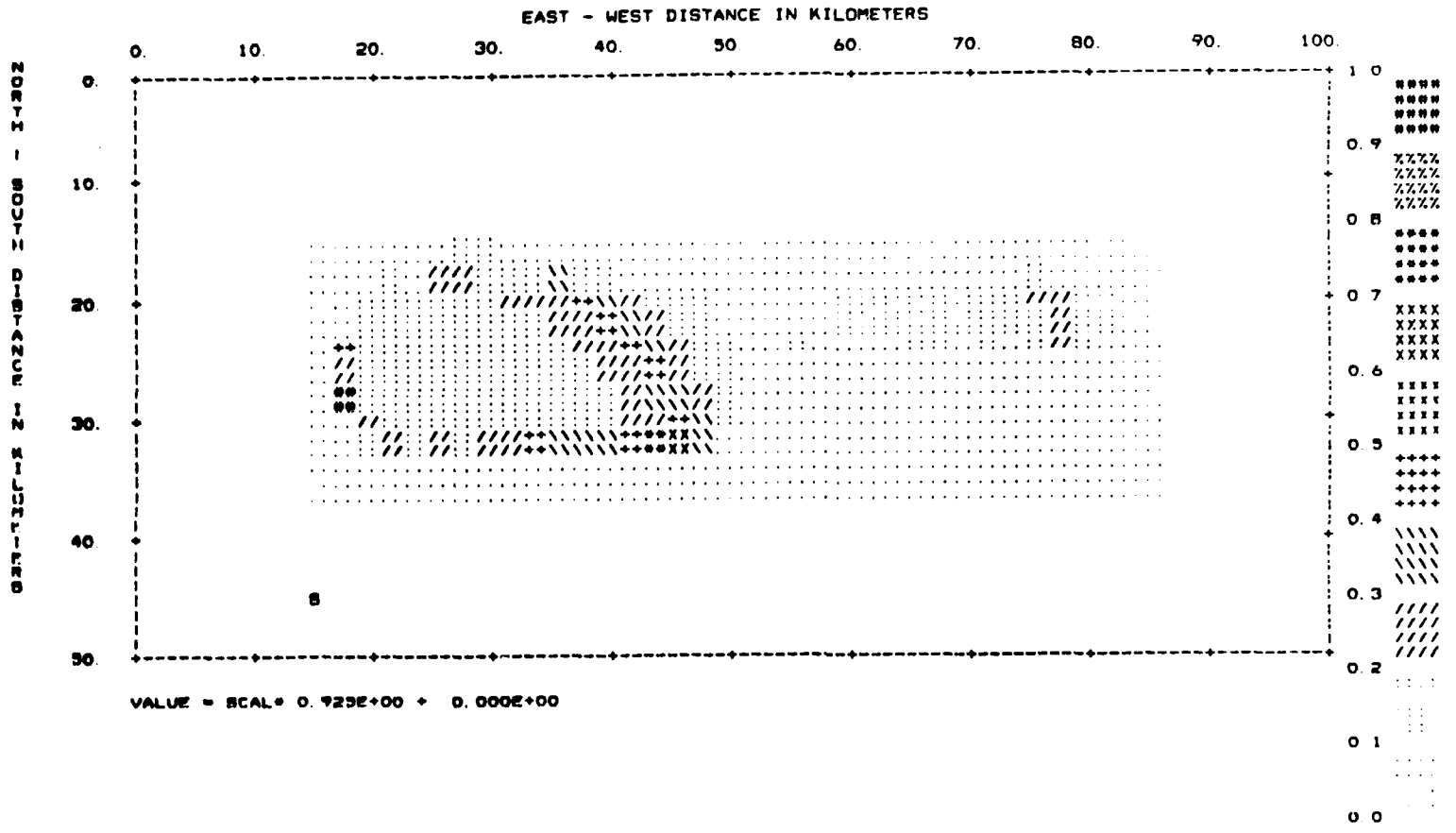
BASIN MODEL 4
PERIOD = 1 0000 SECONDS
EAST - WEST DISTANCE IN KILOMETERS
0. 10. 20. 30. 40. 50 60. 70. 80. 90. 100.
NORTH - SOUTH DISTANCE IN KILOMETERS
0. 10. 20. 30. 40. 50.
1 0
0 9
0 8
0 7
0 6
0 5
0 4
0 3
0 2
0 1
0 0
VALUE = SCALE 0. 923E+00 + 0. 000E+00

FIGURE 37

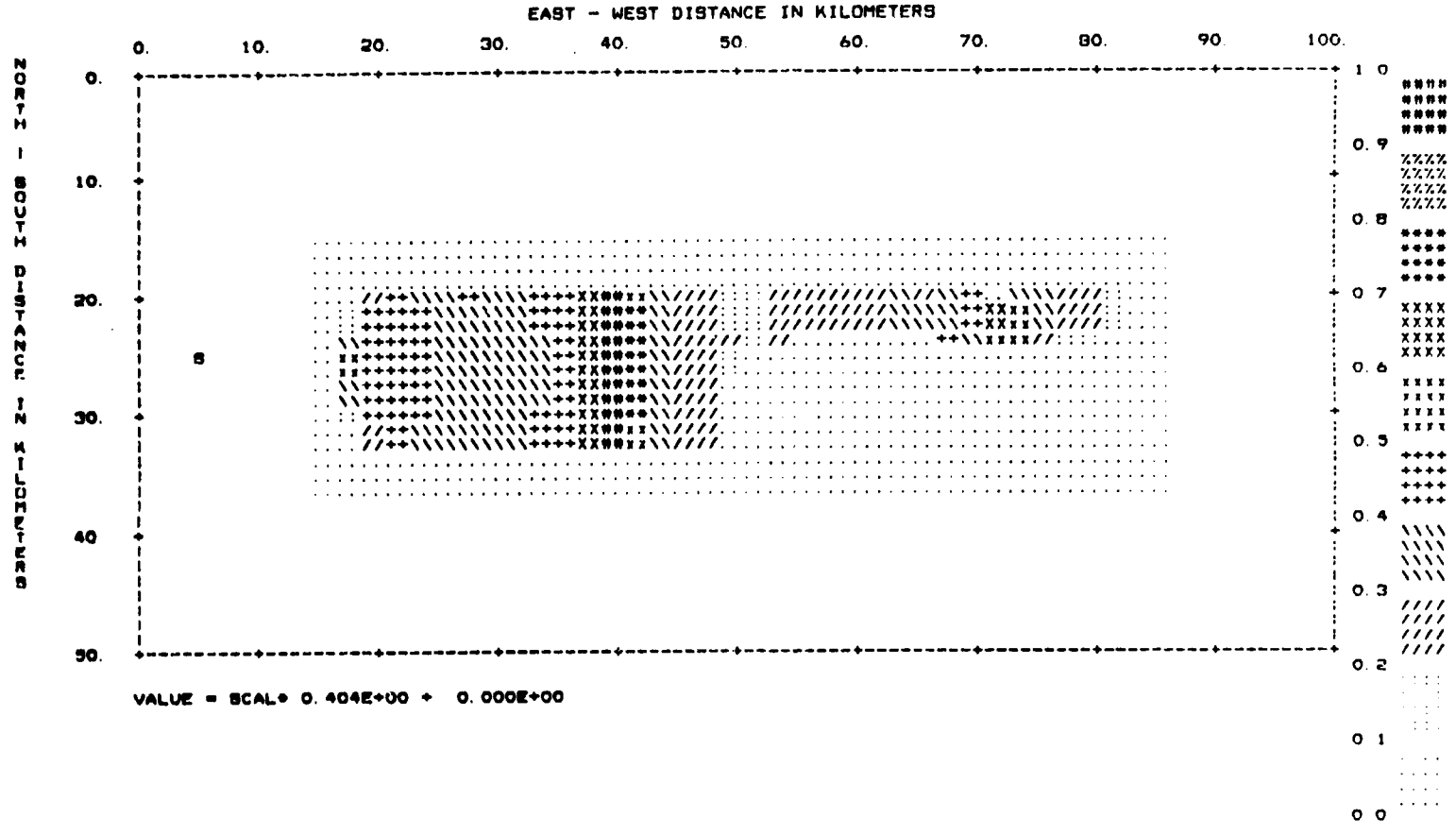
BASIN MODEL 4
PERIOD = 1.0000 SECONDS
EAST - WEST DISTANCE IN KILOMETERS
0. 10. 20. 30. 40. 50. 60. 70. 80. 90. 100.
NORTH - SOUTH DISTANCE IN KILOMETERS
0. 10. 20. 30. 40. 50.
S
1.0 0.9 0.8 0.7 0.6 0.5 0.4 0.3 0.2 0.1 0.0
VALUE = SCALE 0.404E+00 + 0.000E+00

FIGURE 38

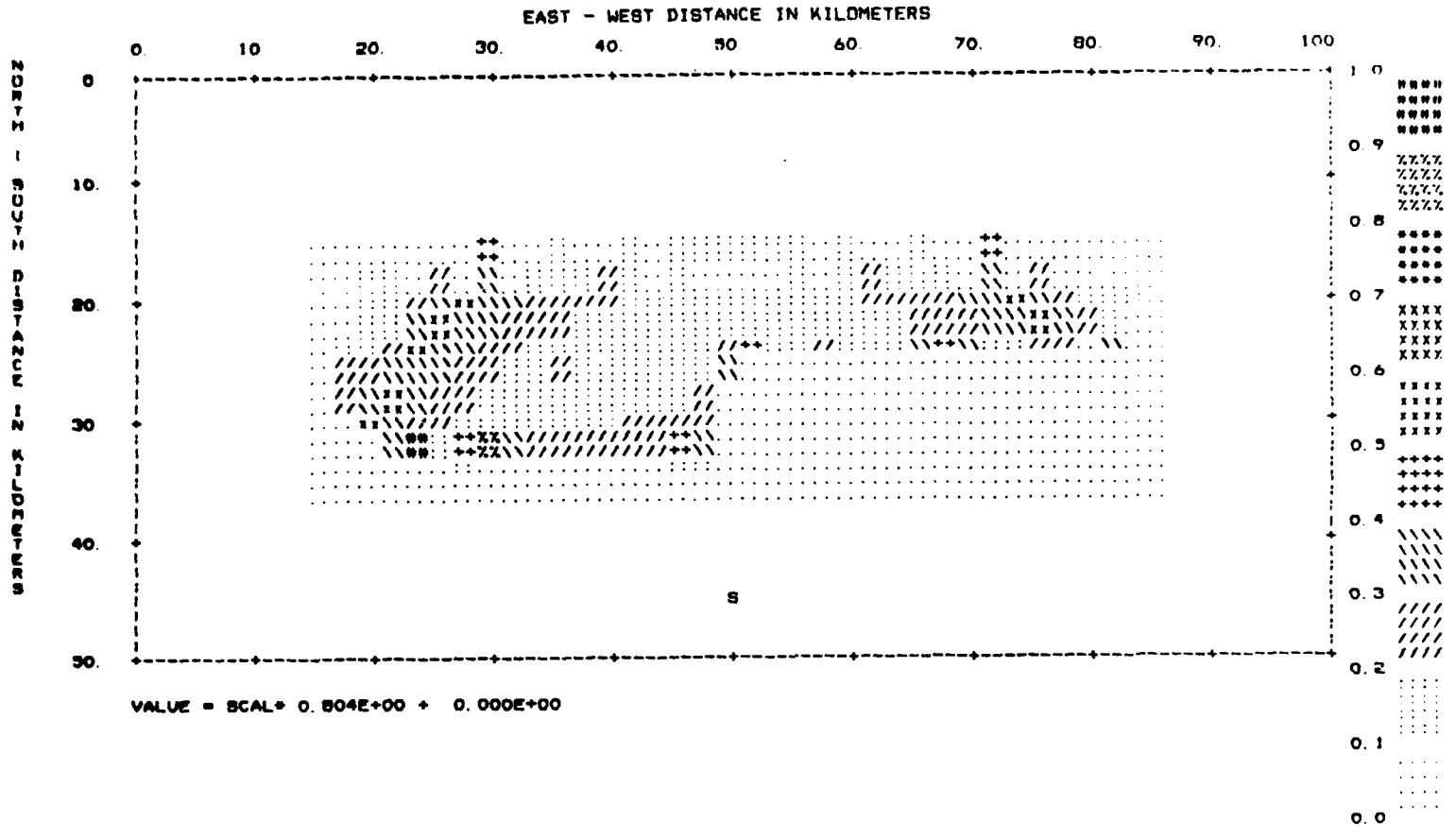
BASIN MODEL 4
PERIOD = 1.0000 SECONDS
EAST - WEST DISTANCE IN KILOMETERS
0.
10
20.
30.
40.
50
60.
70.
80.
90.
100
NORTH - SOUTH DISTANCE IN KILOMETERS
0
10.
20.
30.
40.
50.
S
1.0
0.9
0.8
0.7
0.6
0.5
0.4
0.3
0.2
0.1
0.0
VALUE = SCALE 0.804E+00 + 0.000E+00

FIGURE 39

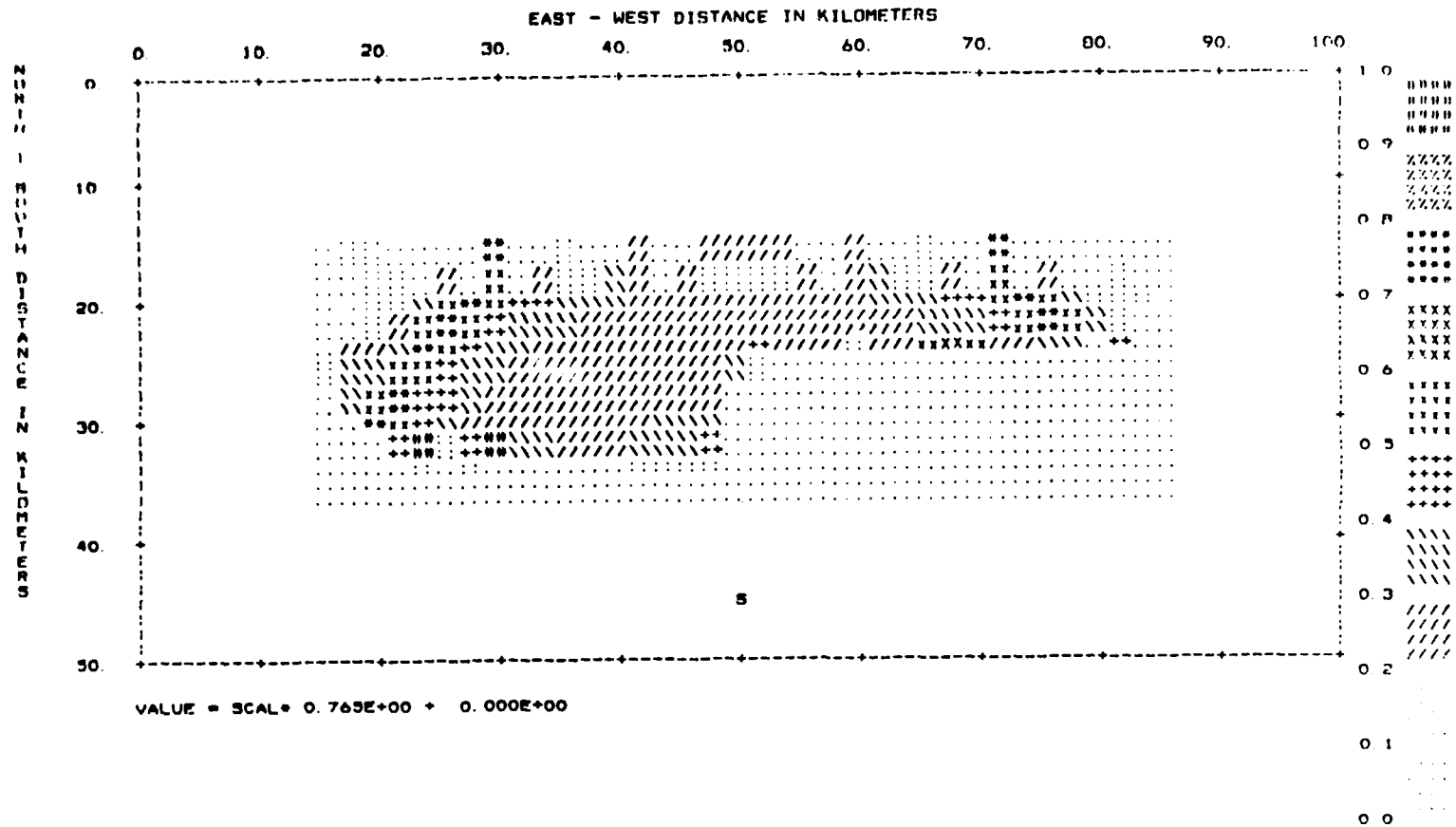
BASIN MODEL 4
PERIOD = 0.0625 SECONDS
EAST - WEST DISTANCE IN KILOMETERS
0
10.
20.
30.
40.
50.
60.
70.
80.
90.
100
NORTH - SOUTH DISTANCE IN KILOMETERS
0
10
20.
30.
40.
50.
1.0
0.9
0.8
0.7
0.6
0.5
0.4
0.3
0.2
0.1
0.0
S
VALUE = SCALE 0.765E+00 + 0.000E+00

FIGURE 40

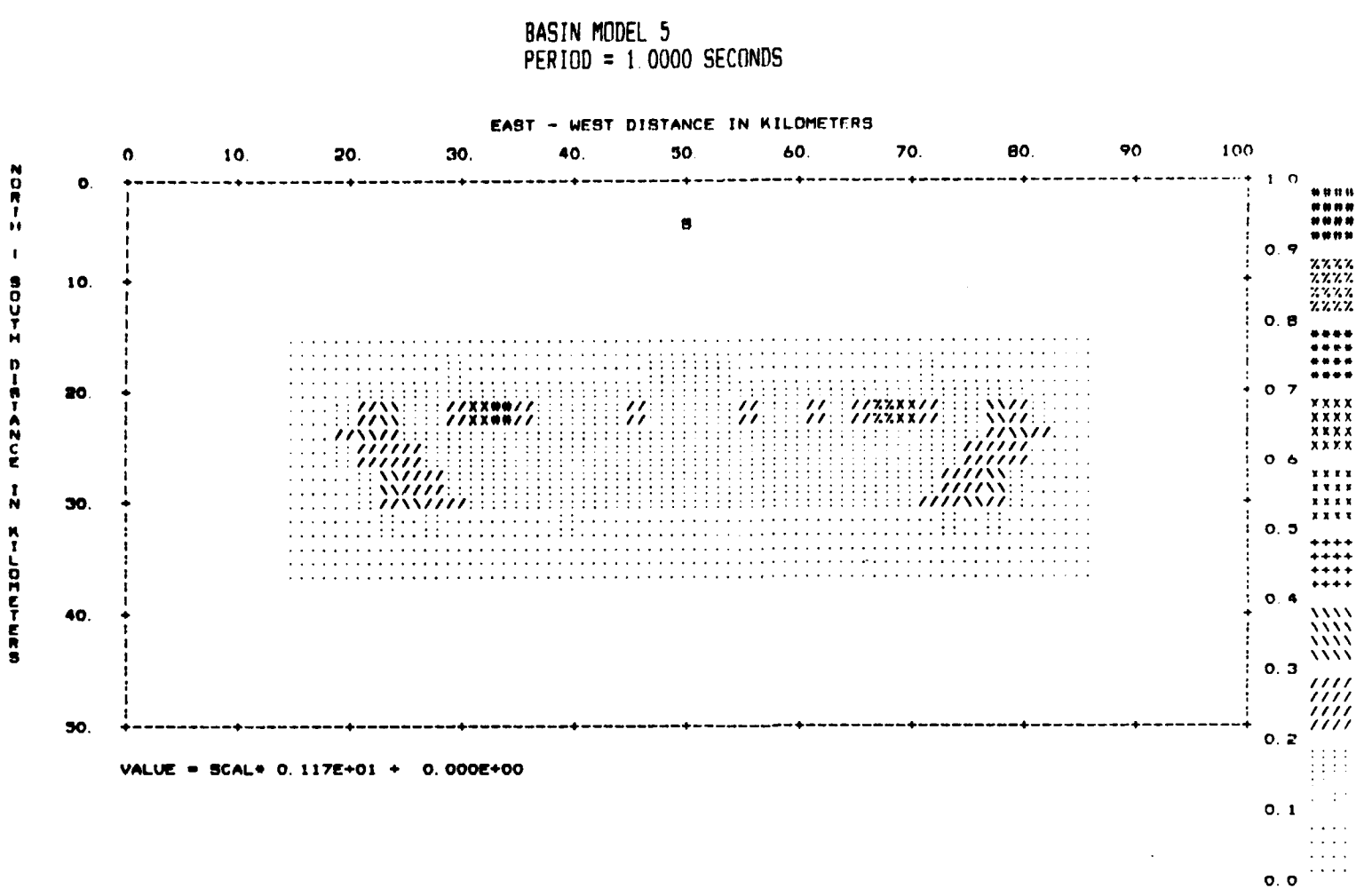
BASIN MODEL 5
PERIOD = 1.0000 SECONDS
EAST - WEST DISTANCE IN KILOMETERS
0
10.
20.
30.
40.
50
60.
70.
80.
90
100
NORTH - SOUTH DISTANCE IN KILOMETERS
0.
10.
20.
30.
40.
50.
1.0
0.9
0.8
0.7
0.6
0.5
0.4
0.3
0.2
0.1
0.0
VALUE = SCAL* 0.117E+01 + 0.000E+00

FIGURE 41

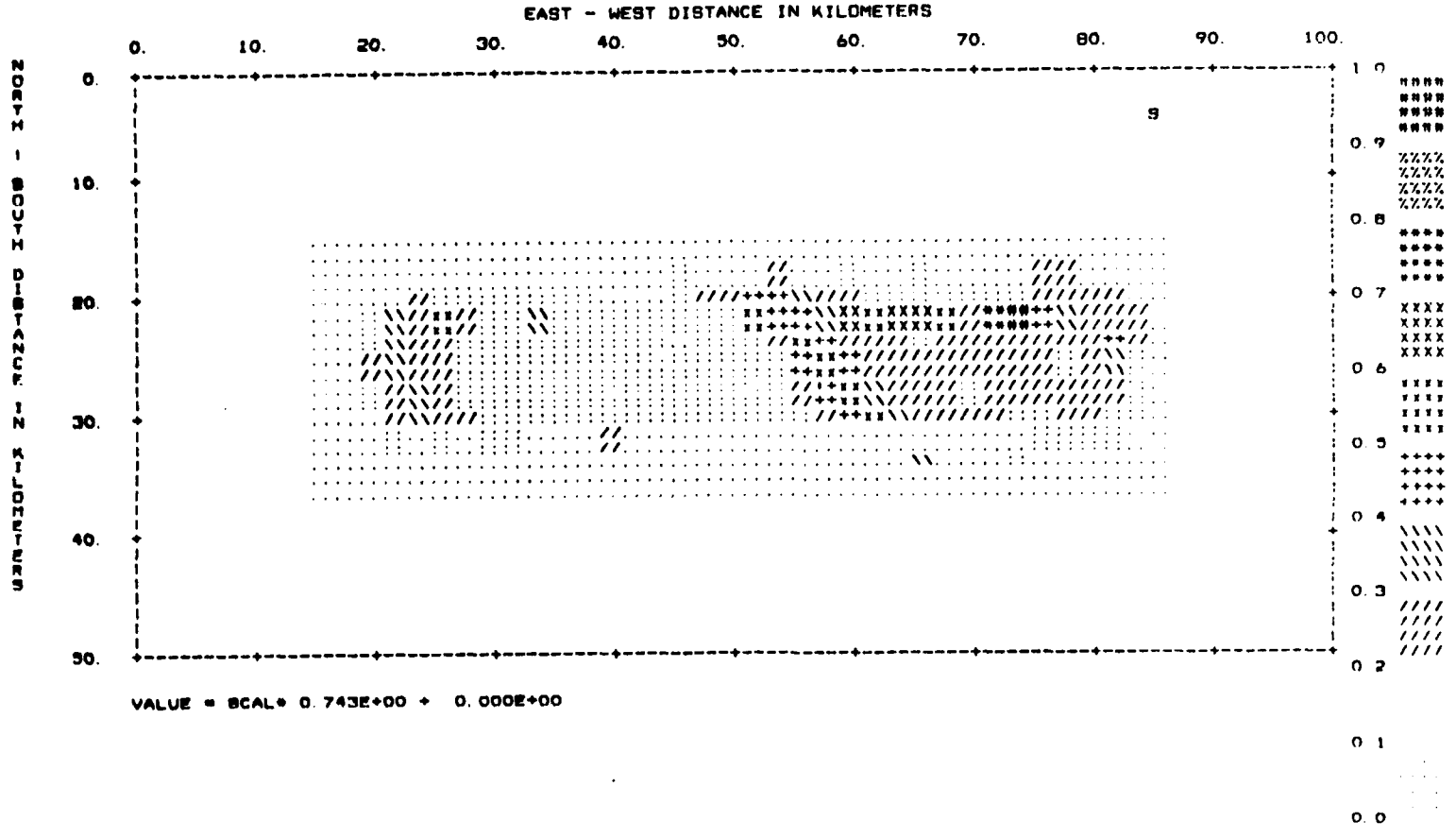
BASIN MODEL 5
PERIOD = 1.0000 SECONDS
EAST - WEST DISTANCE IN KILOMETERS
0. 10. 20. 30. 40. 50. 60. 70. 80. 90. 100.
NORTH - SOUTH DISTANCE IN KILOMETERS
0. 10. 20. 30. 40. 50.
1.0 0.9 0.8 0.7 0.6 0.5 0.4 0.3 0.2 0.1 0.0
VALUE = SCALE 0.743E+00 + 0.000E+00

FIGURE 42

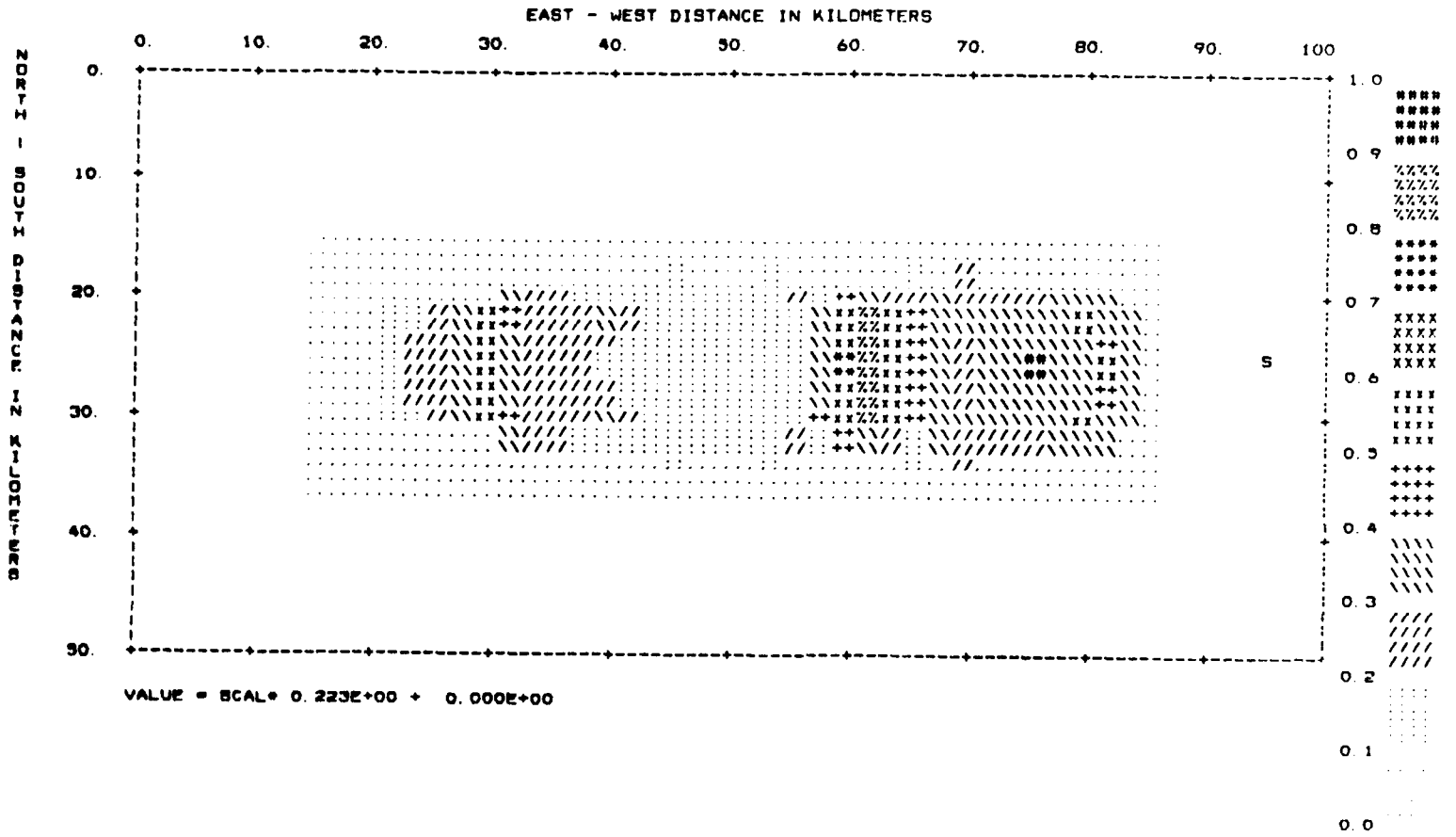
BASIN MODEL 5
PERIOD = 2.0000 SECONDS
EAST - WEST DISTANCE IN KILOMETERS
0. 10. 20. 30. 40. 50. 60. 70. 80. 90. 100
NORTH - SOUTH DISTANCE IN KILOMETERS
0. 10. 20. 30. 40. 50.
1.0 0.9 0.8 0.7 0.6 0.5 0.4 0.3 0.2 0.1 0.0
S
VALUE = SCALE 0.223E+00 + 0.000E+00

FIGURE 43

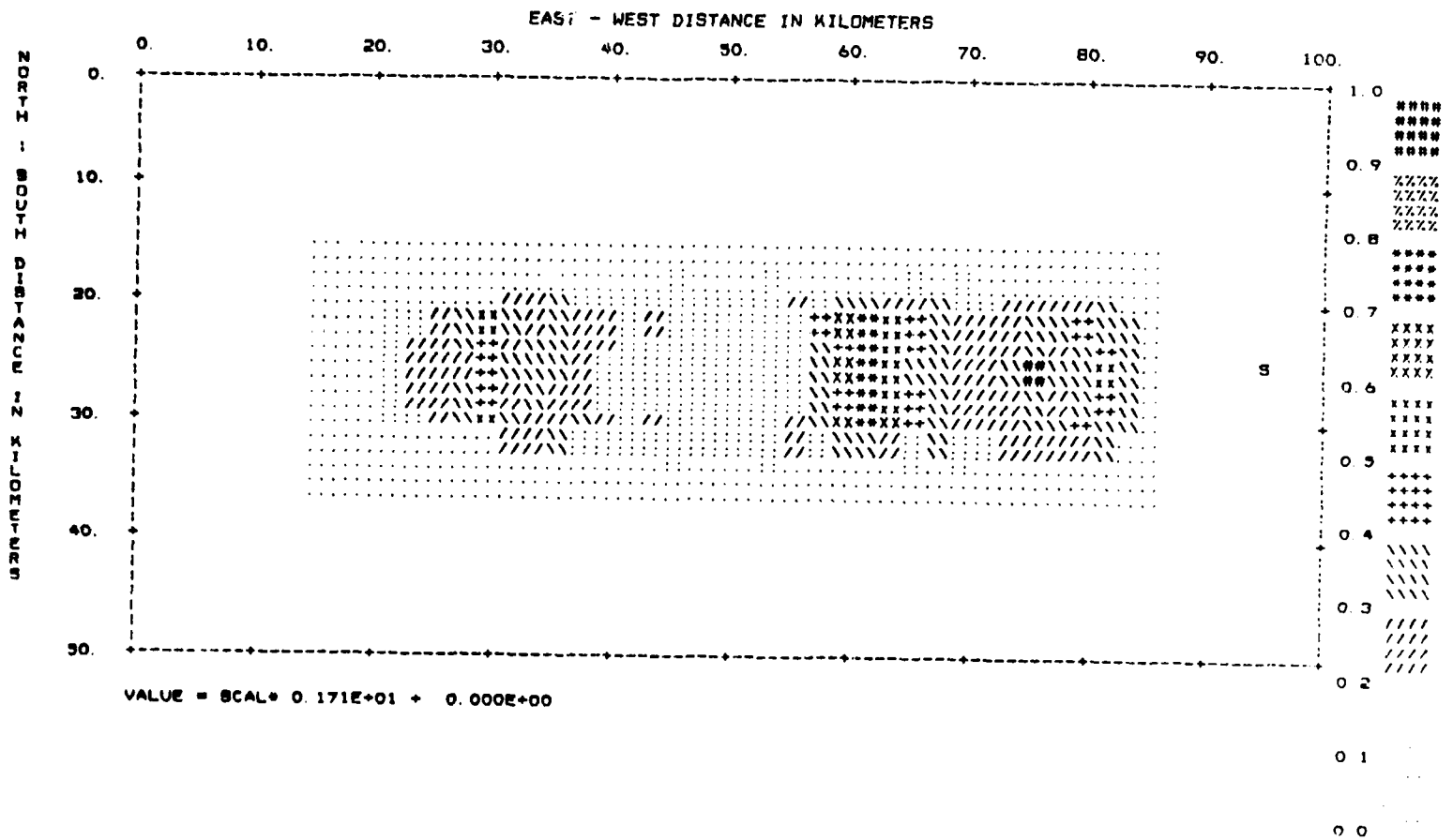
BASIN MODEL 5
PERIOD = 0.5000 SECONDS
EAST - WEST DISTANCE IN KILOMETERS
0. 10. 20. 30. 40. 50. 60. 70. 80. 90. 100.
NORTH - SOUTH DISTANCE IN KILOMETERS
0. 10. 20. 30. 40. 50.
S
1.0 0.9 0.8 0.7 0.6 0.5 0.4 0.3 0.2 0.1 0.0
VALUE = SCALE 0.171E+01 + 0.000E+00

FIGURE 44

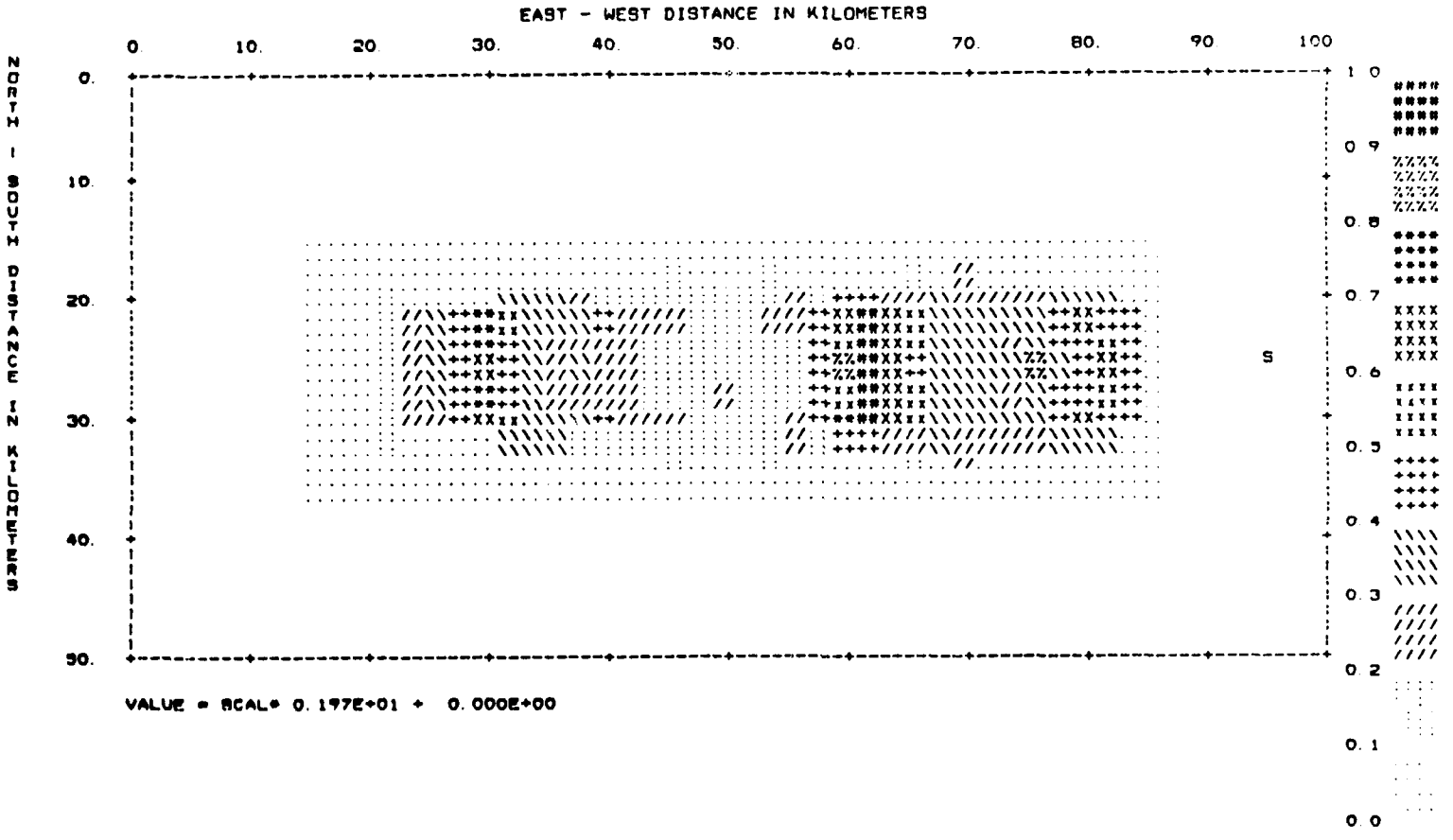
BASIN MODEL 5
PERIOD = 0.1250 SECONDS
EAST - WEST DISTANCE IN KILOMETERS
0
10.
20.
30.
40.
50.
60.
70.
80.
90
100
NORTH - SOUTH DISTANCE IN KILOMETERS
0.
10.
20.
30.
40.
50.
1.0
0.9
0.8
0.7
0.6
0.5
0.4
0.3
0.2
0.1
0.0
S
VALUE = SCALE 0.197E+01 + 0.000E+00

FIGURE 45

through 45 for three different source locations. All of the focused rays here are Type I arrivals. The most interesting comparison here is to Figures 7, 8, and 9 which have the BASIN 1 results. Most noticeably the long relatively coherent line of high intensity along the sidewall of BASIN 1 from a source to the side is largely gone in BASIN 5 and even what high amplitudes are there are 50% smaller. In the source off the long axis case, the gentler sides of BASIN 5 serve to spread the areas of high intensity out by a factor of 2 to 3.

4.0 SUMMARY

A number of general observations can be drawn from this preliminary analysis with regard to the effects of varying certain generic basin parameters. For example, we note that the typical steep basin sides (averaging 60° dips) in the Basin and Range province tend to cause concentrations of high intensity ground motion along the edges of the basins. Moreover, the ends of basins seem to carry substantial risk of high amplitude motion. Roughness in the principal interfaces in a basin, not surprisingly, tends to scatter seismic energy. The spectral distribution of that scattered energy is a function of the scale size of the scatterers. Hence, random roughness at scale lengths comparable to the seismic wavelengths of interest will minimize strong focus points. From the standpoint of minimizing strong ground motion at a particular site, the surrounding geologic structures should be examined to insure that the site is not uniformly biased towards high ground motions as a result of natural focuses. Certainly potential ground motions at sites within basins is reduced (aside from the effects of impedance amplification) as the geologic structures, as seen by the first few multiple bounce rays, approximates a flat layered model.

These modeling studies will form significant foundation for the analysis of realistic basin models. A complete discussion of such an analysis will be presented in the final technical report together with a detailed discussion of the theoretical and mathematic basis of three dimensional seismic raytracing for strong ground motion studies.

5.0 REFERENCES

Battis, J.C., Seismic velocity models for western alluvial basins, Air Force Geophysics Laboratory Report No. AFGL-TR-81-0139, 1981, ADA108153.

Cerveny, V., M.M. Popov, and I. Psencik, Computation of seismic wave fields in inhomogeneous media - Gaussian beam approach, submitted to Geophys. J.R. astr. Soc., 1982.

END

DATE
FILMED

1-84

DTIC